

Aus der Universitätsklinik für Allgemeine, Viszeral- und
Transplantationschirurgie Tübingen

**Optimization of the spatial distribution
of a therapeutic pressurized aerosol (PIPAC):
an ex-vivo study**

Inaugural-Dissertation
zur Erlangung des Doktorgrades
der Medizin

der Medizinischen Fakultät
der Eberhard Karls Universität
zu Tübingen

vorgelegt von
Schnelle, Daniel Patrick

2020

Dekan: Professor Dr. I. B. Autenrieth

1. Berichterstatter: Professor Dr. A. Königsrainer

2. Berichterstatterin: Professorin Dr. K. Schenke-Layland

Tag der Disputation: 20. Februar 2020

Table of contents

I	List of abbreviations.....	6
II	List of tables.....	7
III	List of figures.....	8
1	Introduction.....	10
1.1	The Peritoneum – barrier and carrier	13
1.2	Peritoneal metastasis	14
1.3	Pressurized Intraperitoneal Aerosol Chemotherapy (PIPAC).....	14
1.3.1	Principle.....	14
1.3.2	Technological setting	15
1.3.3	Postulated advantages	17
1.3.4	Current evidence – state of the art.....	18
1.3.5	Limitations	22
1.3.6	Side effects of chemotherapy	22
1.4	Physical parameters.....	24
1.4.1	Aerosol	24
1.4.2	Distribution pattern.....	26
1.4.3	Drug concentration	27
1.4.4	Hydrostatic pressure within the abdominal cavity	28
1.4.5	Depth of drug tissue penetration.....	29
1.5	Scientific problem	29
2	Methods	31
2.1	Ethical and regulatory framework.....	31
2.2	Study design	31
2.3	In-vitro models.....	32
2.3.1	Granulometric analysis	32
2.3.2	Thermographic Imaging.....	33
2.4	Ex-vivo models.....	35
2.4.1	Inverted bovine urinary bladder	35
2.4.2	Medical devices	36

2.4.3	Distribution experiments with Methylene Blue (visual examination)	39
2.4.4	Distribution experiments with ICG (macroscopy) and DAPI (microscopy)	40
2.4.5	Distribution experiments with Cisplatin (tissue concentration)	43
2.5	Occupational health safety aspects	44
2.6	Statistics	44
3	Results	45
3.1	Granulometric analysis	45
3.2	Thermographic Imaging	46
3.2.1	Results of Thermographic Imaging	46
3.2.2	Description of the thermographic images	48
3.2.3	Comparison of properties of Capnopen® and Prototype4	50
3.3	Inverted bovine urinary bladder experiments	51
3.3.1	Distribution experiments with methylene blue (visual examination)	51
3.3.2	Distribution experiments with ICG (macroscopy)	51
3.3.3	Distribution experiments with DAPI (microscopy)	56
3.3.4	Distribution experiments with Cisplatin (tissue concentration)	61
4	Discussion	63
4.1	Development and validations of preclinical models	63
4.1.1	Inverted bovine bladder model: characteristics and advantages over existing preclinical models	63
4.1.2	Inverted bovine bladder model: limitations	65
4.1.3	Thermographic Imaging model	66
4.2	Evaluation of a next-generation medical device	68
4.2.1	Granulometric analysis	69
4.2.2	Injection angle and distribution velocity	70
4.2.3	Visual examination of distribution pattern	70
4.2.4	Penetration depths in inverted bovine urinary bladder model	72
4.3	Conclusion	75
5	Abstract	78

6	Zusammenfassung (Deutsch)	80
7	References	83
8	Declaration of authorship	89
9	Publications	90
10	Acknowledgement	91

I List of abbreviations

AAS	Atomic Absorbance Spectroscopy
CAWS	Closed Aerosol Waste System
CTCAE	Common Terminology Criteria for Adverse Events
CRS	Complete Radical Surgery
CT	Computer Tomography
DAPI	4',6-Diamidino-2-Phenylindole
Dv(x)	Diameter Value
FDA	Food and Drug Administration
gGT	Gamma Glutamyl Transferase
GOT	Glutamic Oxaloacetic Transaminase
GPT	Glutamic Pyruvic Transaminase
HEPA Filter	High Efficiency Particulate Air Filter
HIPEC	Hyperthermic Intraperitoneal Chemotherapy
ICG	Indocyanine Green
Max	Maximum
µm	Mikrometer
Min	Minimum
PM	Peritoneal Metastasis
PMI	Peritoneal Metastasis Index
PCI	Peritoneal Cancer Index
PIPAC	Pressurized Intraperitoneal Aerosol Chemotherapy
Stand Dev	Standard Deviation

II List of Tables

Table 1: Injection parameters for Thermographic Imaging	34
Table 2: Solution formulations of inverted bovine urinary bladder experiments	38
Table 3: Aerosol formulation and application parameters of ICG/DAPI experiments.....	40
Table 4: Aerosol formulation and application parameters of Cisplatin experiments	43
Table 5: Comparison of different diameter values ($D_v(10)$, $D_v(50)$, $D_v(90)$).....	45
Table 6: Temperature levels of Thermographic Imaging	47
Table 7: Comparable aerosol distribution snapshots.....	50
Table 8: Characteristics of ICG aerosolized bladders (Capnopen®)	53
Table 9: Characteristics of ICG aerosolized bladders (Prototype4).....	55
Table 10: Summary of penetration depth results (Capnopen®)	57
Table 11: Summary of penetration depth results (Prototype4)	59
Table 12: Summary of tissue concentration results.....	61
Table 13: Characteristics of different experimental approaches for pressurized aerosol optimization	65

III List of Figures

Figure 1: Schematic PIPAC operational setting.....	16
Figure 2: Quality by Design concept applied to the process of PIPAC procedure	27
Figure 3: Experimental setup of the SprayTec® droplet analyzer	32
Figure 4: Experimental setup of Thermographic Imaging experiments	34
Figure 5: Experimental setup of the inverted bovine urinary bladder experiments.	37
Figure 6: Medical devices: Capnopen® and the newest generation, Prototype4	37
Figure 7: Interior view of a sliced inverted bovine urinary bladder after sample removal	39
Figure 8: IC-View Camera	41
Figure 9: Schematic selection of three representative sections in a tissue sample	42
Figure 10: Exemplary image of penetration depth measurements with fluorescence microscopy.....	42
Figure 11: Particle diameter distribution of Capnopen® and Prototype4.....	45
Figure 12: Thermographic Imaging during injection period into model box	48
Figure 13: Injection angles of Capnopen® (left) and Prototype4 (right).....	50
Figure 14: Overview of the stained bovine urinary bladders after opening.....	51
Figure 15: Photo documentation of ICG-sprinkled bladders with the Capnopen®	52

Figure 16: Photo documentation of ICG-sprinkled bladders with the Prototype4 54

Figure 17: Graphic representation of different penetration depths depending on the position in the bladder (Capnopen®)..... 56

Figure 18: Graphic representation of different penetration depths depending on the position in the bladder (Prototype4)..... 58

Figure 19: Graphic representation of different penetration depths depending on the position in the bladder using Prototype4. 58

Figure 20: Penetration depths of Capnopen®/Prototype4 sorted by regions ... 60

Figure 21: Tissue concentration of Cisplatin sorted by regions (Capnopen®).. 61

1 Introduction

For a long time, peritoneal metastasis (PM) has been considered to be a terminal clinical condition without any possible curative therapeutic approach (Weber et al., 2012). Patients suffering from different cancer types combined with PM were only treated with palliative intravenous systemic chemotherapy; the results were limited, for example with a median survival period of 5-7 months in patients with PM of colorectal origin (Jayne et al., 2002). Gradually, as new chemotherapeutic drugs and biological agents were developed, treatment options of PM have been enlarged. However, the median survival rates of 16 months for colorectal cancer (Franko et al., 2016), 7 – 10 months for gastric cancer (Rivera et al., 2007), 4 – 10 months for ovarian cancer (Hanker et al., 2012) and 6 – 12 months for peritoneal mesothelioma (Chua et al., 2009), are still not satisfying.

In 1996, Sugarbaker suggested to overthink the point of view upon current understanding of cancer spreading, establishing the idea of considering PM as a locally advanced disease, if metastases in other organs could be excluded (Sugarbaker, 1996). Thus, in the last three decades, a new multimodal approach to deal with PM has been established, combining Complete Cytoreductive Surgery (CRS) with Hyperthermic Intraperitoneal Chemotherapy (HIPEC) and possibly systemic chemotherapy. The idea is to remove the entire visible tumor tissue and then fill the abdominal cavity with a heated chemotherapeutic solution in order to erase microscopic tumoral remains, which are still present after surgery and are responsible for the relapse of PM (Losa et al., 2014, Sugarbaker, 2016). There is a consensus that CRS and HIPEC should only be offered to highly selected patients (Weber et al., 2012). The decision for applying this combination takes into consideration the extent of disease, as measured by the Peritoneal Cancer Index (PCI), the tumor type and the general condition of the patient, quantified by means of the Karnofsky performance status scale (Beckert et al., 2016). Diffuse small bowel infiltration has to be regarded as a contraindication due to the fact that, through CRS, a too short vital small bowel segment would be left, which is incompatible with life (Marmor et al., 2016). In addition to that, this treatment strategy is hampered by significant risks and side effects (Gill et al.,

2011). Despite these limitations, in clinical practice, CRS + HIPEC is commonly performed and is established as the standard therapeutic approach to selected patients with PM from various original tumor locations (Losa et al., 2014, de Cuba et al., 2013, Sugarbaker, 2016).

In the past, chemotherapy has been exclusively administered intravenously. However, it has been shown, that loco-regional delivery is associated with a better therapeutic ratio, namely a high local drug concentration and a lower systemic exposure resulting in less toxicity (Markman, 2003). However, classical methods for delivering intracavitary chemotherapy are hampered by pharmacological limitations (Ceelen and Flessner, 2010). These limitations include in particular a poor penetration into the tissue and an inhomogeneous distribution pattern (Dedrick and Flessner, 1997). A particular problem is the elevated interstitial pressure in tumor tissue, which counteracts the effective, deep penetration of therapeutic drugs into the tumor nodules (Heldin et al., 2004).

In the last twenty years, many efforts have been made to develop new strategies for treating PM of various origins. In order to overcome these above mentioned limitations, a new drug delivery system into the peritoneal cavity has been proposed (Reymond et al., 2000), called Pressurized intraperitoneal aerosol chemotherapy (PIPAC). PIPAC is a new innovative approach to treat PM more effectively by administering a pressurized, chemotherapeutic drug containing aerosol into the abdominal cavity. The rationale for this approach is to use the physical characteristics of gas and pressure and closed abdomen physical laws to obtain a more homogeneous drug distribution and a deeper drug penetration into tumoral tissue. Several experimental studies document an increased drug penetration into tissues when a positive hydrostatic pressure is applied, including studies in vitro (Haidara et al 2017), in the rodent (Jacquet et al., 1996, Esquis et al., 2006), in the swine (Facy et al., 2012, Solass et al., 2012b), ex vivo (Solass et al., 2012a) and in vivo (Solass et al., 2012b).

Moreover, it has been shown that aerosolizing of a therapeutic drug into a capnoperitoneum improves homogeneity of drug distribution as compared to intraperitoneal lavage with a liquid solution (Solass et al., 2012b, Solass et al.,

2012a, Sanchez-Garcia et al., 2014, Padilla-Valverde et al., 2016). Presence of drug in tissue has been documented in all compartments of the abdomen (Khosrawipour et al., 2016c). However, this homogeneity is still not ideal, as demonstrated ex vivo (Khosrawipour et al., 2016b, Khosrawipour et al., 2016a) and in the post-mortem swine model (Khosrawipour et al., 2016c).

It must be noted, that in all models above, measurements were performed under static conditions: only the result of application, as determined by tissue concentration or penetration depth at the end of the period of exposition, was measured. This is obviously a significant limitation since aerosol distribution is depending upon time. Due to gravitation forces, any aerosol is expected to sediment after a given period of time. In the present work, a new dynamic, thermographic model, analyzing the injection behavior and the consecutive spatial distribution of the aerosol over time, is introduced with the purpose of filling this particular gap in PIPAC research.

At present, a CE-certified device, the Capnopen® (Capnomed GmbH Villingendorf, Germany) is used as standard in the operational setting for nebulizing the drug containing solution into the abdominal cavity. Various publications have demonstrated, that the spatial distribution of the administered aerosol is still not ideally homogenous (Khosrawipour et al., 2016c, Khosrawipour et al., 2016b) and droplet size still varies to a considerable extent (Gohler et al., 2016) It might be interesting to examine the technical properties and the spraying behavior of the Capnopen® of the next generation (Prototype4). In the present work, these two generations of nebulizers are compared considering the spatial distribution of the aerosol.

Until now, many different preclinical studies have been performed in order to optimize PIPAC technology. In doing so, different models, such as plastic boxes (Khosrawipour et al., 2016a, Solass et al., 2012a, Khosrawipour et al., 2016b), living animals (Solass et al., 2012b) and postmortem swine models (Khosrawipour et al., 2016c) mimicking the abdominal cavity, were used with both advantages and disadvantages. In the present work, the inverted bovine urinary bladder as a new preclinical model is introduced.

1.1 The Peritoneum – barrier and carrier

The peritoneum is a serous membrane consisting of a single layer of mesothelium and a thin layer of connective tissue. It is situated in the abdominal cavity and forms the lining of the abdominal organs such as stomach, liver, spleen, part of the pancreas and the major parts of the small bowel and colon. In women, also the ovaries and fallopian tubes are situated intraperitoneally. The functions of the peritoneum are a leading structure for the nerves, blood vessels and lymph vessels of the abdominal organs and a support of stability by keeping the structure of the abdominal cavity in shape (Reymond and Solass, 2014).

The lining of the inside of the abdominal cavity is called parietal peritoneum, the cover of the organs visceral peritoneum. It must be noted, that only the parietal peritoneum is innervated and thus sensitive to pain. Inflammation of the inner organs or adhesions within in the abdominal cavity can irritate the peritoneum and consecutively cause severe abdominal pain, which is felt vague and difficult to locate.

The complete surface area of the peritoneum is approximately 1.5 - 2 m² (Albanese et al., 2009). The visceral and parietal layers form a potential space between each other, called the abdominal cavity. This is filled with a serous lubricating substance (50ml), which allows both layers to glide smoothly over each other. While laparoscopic interventions, this potential space is inflated with CO₂, forming the capnoperitoneum (Alijani et al., 2004).

In addition to the production of the peritoneal fluid, the peritoneum has also other functions. Specifically, it serves as a defense barrier against intra-abdominal infections and cancer invasion (West et al., 2010).

The peritoneum and its underlying lymphatic system are connected through a multitude of minute orifices. Thus, the free tumor cells tend to deposit on lymphatic spots, from where they infiltrate the beneath lymphatic system. This process primarily takes place on the surface of the diaphragm, the greater omentum, the small intestine mesentery, the epiploic appendices of the large intestine and the pelvic peritoneum. In comparison to that, liver, spleen, or

stomach are affected only in the final stadium of peritoneal disease (Losa et al., 2014).

1.2 Peritoneal metastasis

The extensive infestation of the abdominal lining through malignant cells forming tumor implants is called peritoneal metastasis (PM). The aspect of PM can be very variable. Tumor nodules can vary in size, number and distribution, with or without infiltration into the visceral organs (Chu et al., 1989). In general, they are the consequence of other malignancies such as colon, gastric or ovarian cancer (Halkia et al., 2014).

There are many factors, why PM is difficult to treat and the survival period still unsatisfactory. To begin with, the surface of the peritoneal cavity is large with an area of up to 2.0 m². As some parts of the abdominal cavity are very difficult to reach, liquid intraperitoneal chemotherapy is not able to distribute homogenously within the cavity, leaving tumor tissue remain untreated (Dedrick and Flessner, 1997). Thus, the chemotherapeutic agent applied through intraperitoneal chemotherapy is absorbed inadequately and therefore cannot develop its entire cytotoxic effect. In addition to that, resistance of PM to systemic chemotherapy can also be explained by molecular mechanisms (Griffiths et al., 2011).

1.3 Pressurized Intraperitoneal Aerosol Chemotherapy (PIPAC)

1.3.1 Principle

Pressurized Intraperitoneal Aerosol Chemotherapy (PIPAC) is a new therapeutic approach to treat PM in patients with gastrointestinal and gynecological cancer. The basic idea of PIPAC is to improve the application form of intraperitoneal chemotherapy by creating a drug-containing aerosol, which is administered under pressure into the closed abdominal cavity. Main objective of this new technology is to achieve a more homogeneous distribution of chemotherapeutic agents within the abdominal cavity and a maximum penetration depth into peritoneal tissue (Reymond et al., 2000, Solass et al., 2014).

It must be noted that PIPAC technology combines two basic principles. On the one hand, there is the application form, in which a therapeutic agent is insufflated into the abdominal cavity as a pressurized aerosol. On the other hand, the environment, in which PIPAC is performed, can be steered effectively by modifying physical and chemical parameters. For example, the temperature of the capnoperitoneum, the established pressure and the duration of application can be varied. The optimal combination of the form of drug administration and the environmental properties is the key to therapeutic success.

PIPAC incorporates well-documented approaches of chemotherapeutical treatment. By using the minimally invasive laparoscopy technique, it is possible to repeat PIPAC application several times within a limited period (Solass et al., 2014). Furthermore, this approach is associated with no substantial therapy-related deterioration of quality of life (Odendahl et al., 2015). In addition, the pharmacokinetic advantages of intraperitoneal administration (low systemic toxicity and higher intratumoral concentration) and of the pressurized nebulization (improved penetration and distribution) complete the benefits of this treatment technique (Grass et al., 2017, Solass et al., 2012b, Robella et al., 2016, Solass et al., 2014).

1.3.2 Technological setting

In a first step, a capnoperitoneum is established with a constant pressure of 12mmHg. Then, a 12-mm trocar is placed infraumbilically, through which the Capnopen®, applying the aerosol, is inserted. A 5-mm trocar, situated in the lateral hemiabdomen, provides access for the camera. After tightness of the abdominal cavity is confirmed by indicating no CO₂ flow, the drug containing aerosol is first aerosolized and then applied by the nebulizer and the injector with a constant flow rate of 30 ml/min. The maximum upstream pressure of the high-pressure injector is set at 200 psi (\approx 13.8 bar)(Cazauran et al., 2018). After an exposure time of 30 min, the capnoperitoneum and the chemotherapy aerosol are removed via high-efficiency particulate arrestance filter system.

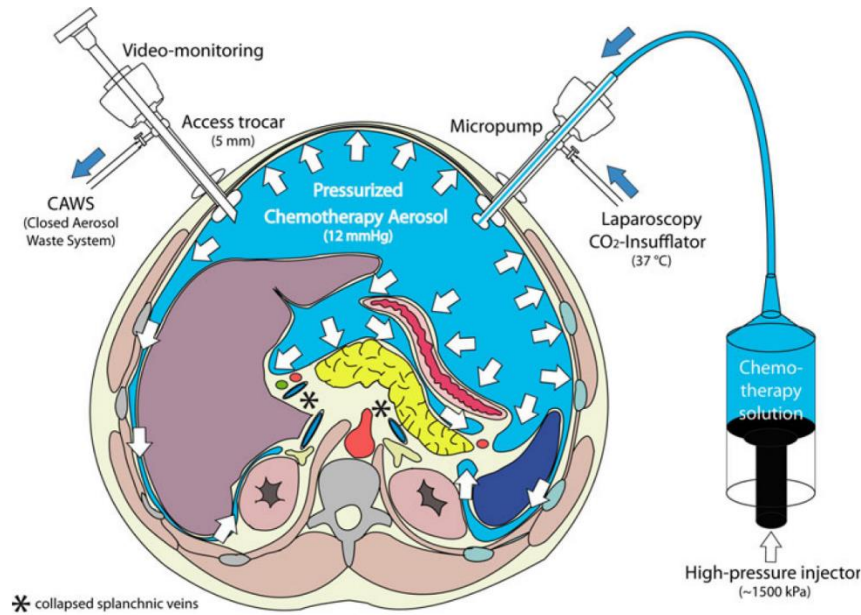


Figure 1: Schematic PIPAC operational setting

A normothermic capnoperitoneum is established with a pressure of 12 mmHg. Then, a chemotherapy solution is aerosolized with a nebulizer and injected into the tightly closed abdominal cavity. After 30 min of maintenance, the toxic aerosol is exhausted through the closed aerosol waste system (CAWS) [adapted from (Solass et al., 2014)].

During exposure time, the surgeon has the possibility to take biopsies of peritoneal lesions.

The process of applying PIPAC technology has been determined using clinically established values. These include the capnoperitoneum of 12 mmHg, the Capnopen® position at a distance of 8 cm to the peritoneal surface of the small intestine and the present formulation of the drug, as an aqueous solution. The influence of these established parameters on the penetration depth of a therapeutic drug (in this case doxorubicin) in the target tissues has recently been investigated in an ex vivo model (Khosrawipour et al., 2016b). In this experiment, distance between the nozzle of the nebulizer and the sample located on the opposite site of the box (spray jet sample) was varied within a range of 2 to 8 cm and its influence on penetration depth was evaluated. The results revealed that the mean penetration depth was higher the closer the nebulizer was located towards the spray jet sample. Interestingly, in all other samples located on the

wall, the bottom cover and the top, penetration depth was registered to be lower the closer the nebulizer was brought to the spray jet sample (Khosrawipour et al., 2016b). Concerning doxorubicin concentration, a higher concentration induces relevant increase of penetration depth in the spray jet sample, but only marginal change in the other peripheral samples. An increase of pressure did not show any relevant increase of penetration depth in any of the samples, including the spray jet one (Khosrawipour et al., 2016b).

1.3.3 Postulated advantages

PIPAC has a substantial pharmacological advantage compared to other intraperitoneal chemotherapy concepts such as HIPEC or catheter-based intraperitoneal chemotherapy. PIPAC can be applied repetitively and does not need CRS in advance. It might be more effective to achieve control of peritoneal residuals because the period in which tumoral tissue is exposed to chemotherapeutic drugs can be expanded to several months (Tempfer et al., 2015b). Many studies have verified, that repeated application of this new method is tolerated very well with justifiable side effects (Nadiradze et al., 2016, Demtroder et al., 2016, Tempfer et al., 2015b, Solass et al., 2014) (Grass et al., 2017).

Another advantageous aspect of the PIPAC technology is to measure repetitively the outcome of antitumor treatment. During PIPAC application, the surgeon enters the abdominal cavity through laparoscopy. This allows him to take tissue samples out of specific regions of the abdominal cavity each time PIPAC is performed. In this way, the effectiveness of chemotherapeutic application can be directly judged by comparing both the PMIs, which are created in each session of PIPAC, and the histologic specimens removed (Solass et al., 2016).

In tumoral tissue, increased intratumoral pressure caused by various mechanism (see below) leads to decreased influx of drugs into the tissue (Heldin et al., 2004). By establishing a capnoperitoneum with a positive pressure of 12 mmHg during PIPAC, this important limiting factor for drug uptake is opposed effectively (Reymond et al., 2000).

PIPAC offers a new possibility of treatment for patients in a salvage situation, in which usually intravenous palliative chemotherapy has only limited efficacy. In the last few years, PIPAC has been introduced as a new approach to treat PM in patients with colorectal, gastric, and ovarian cancer. In patients not eligible for CRS and HIPEC, this new approach delivered promising results concerning the regression of tumor nodule size (Tempfer et al., 2015b, Demtroder et al., 2016, Nadiradze et al., 2016). Yet, an important issue in stratifying the therapy in patients with PM is to stage the dissemination of the disease and then evaluate if CRS and HIPEC can be applied or not. There are cases, where CRS and HIPEC is not possible due to an already large dissemination as indicated by a high Peritoneal Cancer Index (PCI) (Sugarbaker and Jablonski, 1995). Patients with diffuse small bowel involvement cannot be treated with this combination method either (Marmor et al., 2016). In these cases, PIPAC offers a new possibility of “neoadjuvant” treatment. In a pilot study, Girshally et al recently reported the possibility of applying PIPAC for decreasing the diffuse peritoneal spreading to a more localized tumor involvement, so that the criteria for CRS and HIPEC will be met (Girshally et al., 2016). Yet, these first promising results have not been confirmed by randomized phase II/III trials.

1.3.4 Current evidence – state of the art

In the last few years, several experimental (including in vivo, ex vivo and postmortem experiments) and clinical studies have been published with the aim of investigating both the basic pharmacokinetic and pharmacodynamic principles of PIPAC technology and the efficacy, safety, and feasibility of PIPAC procedures in the clinical background.

In 2000, Reymond et al. for the first time described the concept of a therapeutic capnoperitoneum, but technical limitations impeded further clinical development (Reymond et al., 2000). Twelve years later, Solass et al. published the first data about PIPAC technology. In an functioning swine model, distribution of methylene blue within the abdominal cavity was investigated by assessing the stained peritoneal surface at autopsy. Hereby, stained peritoneal surface was larger using the PIPAC technology compared with peritoneal lavage. Furthermore,

staining appeared more intense and hidden peritoneal regions were only reached by methylene blue through the pressured spraying (Solass et al., 2012b).

In another preclinical model, a nontoxic therapeutic agent (Dbait, i.e. noncoding DNA fragments) was aerosolized under pressure into a box containing diseased human peritoneum. Dbait were coupled to cholesterol molecules to facilitate intracellular uptake and to Cyanine to be detected by fluorescence (Solass et al., 2012b). Conventional lavage containing the same agents was applied to the control group. In fluorescence microscopy, penetration depth of 1mm into the tumor was achieved in the nebulized sample, but no fluorescence activity was detected after conventional lavage. In addition to that, detection of histone gamma-H2AX indicated activation of DNA-dependent protein kinase by Dbait and therefore a biological, cytotoxic effect (Solass et al., 2012a).

As the next consecutive step, PIPAC was first applied in November 2011 in three end-stage patients with PM from gastric, appendiceal and ovarian origin, who had already undergone intravenous chemotherapy. In this small case series, the objective was to examine the distribution pattern, histological response, possible side effects and feasibility of the technology. No serious side effects ≥ 2 according to the Common Terminology Criteria for Adverse Events (CTCAE) were observed. Furthermore, the procedure could be carried out without any major obstacles and early hospital discharge was possible. On a histological basis, three patients had a histological remission (two of them complete, one partial) (Solass et al., 2014).

During the further development of PIPAC, not only efficacy and safety were the issues to be investigated, but also particular attention was paid to the spatial drug distribution pattern. For this, PIPAC was performed in an ex-vivo model containing native fresh tissue samples of swine peritoneum. Aim of this study was to understand the drug distribution in space and penetration depth into the located tissue. Here, the results revealed an unequal penetration depth of doxorubicin in the different samples with a significantly higher depth in tissue directly exposed to the device jet (Khosrawipour et al., 2016a).

In the currently standard clinical setting of PIPAC, there are several parameters, including Capnopen® position, pressure, formulation of chemotherapeutic drug containing solution, time period of application and selection of suitable chemotherapeutics, which influence the drug distribution pattern and the penetration depth. For a better understanding of the effect of the position of the Capnopen®, the internal pressure and the doxorubicin dosage, Khosrawipour et al. designed an ex-vivo experiment model, in which these parameters were evaluated (Khosrawipour et al., 2016b). In another experiment, the penetration depth of doxorubicin after PIPAC application was examined in a postmortem swine model (Khosrawipour et al., 2016c). On a more physical basis, Göhler et al. described the technical properties of the Capnopen® and the granulometric characterization of the aerosol (Gohler et al., 2016).

Based on the first data indicating a good safety of PIPAC, the technology has then been evaluated in patients with recurrent PM of various origins. Several studies reported clinical outcomes in patients with PM from colorectal, gastric, and ovarian cancer and PMP (Tempfer et al., 2014a, Tempfer et al., 2014b, Tempfer et al., 2015b, Demtroder et al., 2016, Solass et al., 2014, Giger-Pabst et al., 2018).

The design of these clinical studies was diverse, consisting of prospective case series (Tempfer et al., 2014a, Solass et al., 2014), retrospective studies (Robella et al., 2016, Nadiradze et al., 2016, Demtroder et al., 2016, Girshally et al., 2016), a cohort study (Tempfer et al., 2015a) and case-reports (Giger-Pabst et al., 2015) (Tempfer et al., 2014b).

In the prospective single-arm phase-II study, Tempfer et al assessed the safety and activity of PIPAC technology in women with recurrent ovarian cancer. 62% of the enrolled patients responded significantly to the treatment, 76% showed histologic regression and PM Index improvement. Side effects were tolerable with CTCAE no higher than 3. Moreover, common toxic effects of chemotherapy, as for example nausea/vomiting, appetitive loss, constipation, diarrhea, were reported to improve during therapy. Overall, these results in ovarian cancer were promising and confirmed by various retrospective cohort investigating objective

tumor response and histological regression in patients with recurrent PM of various gastrointestinal and gynecological origins (Tempfer et al., 2015b).

As the current standard drug concentrations in PIPAC therapy are relatively low, it is important to evaluate, whether the current satisfactory tolerability of the treating regime is because of the low systemic uptake or the low drug doses applied (Grass et al., 2017). Tempfer et al. showed, that no dose limiting toxicities were found after escalating the dose of doxorubicin and cisplatin from 1.5mg/m² to 2.1 mg/m² (respectively 7.5mg/m² to 10.5 mg/m²) (Tempfer et al., 2018).

At the moment, on ClinicalTrials (clinicaltrials.gov), five further phase-II trials can be identified:

- An open-label, single-arm trial investigating the feasibility, safety, tolerability, preliminary efficacy, costs, and pharmacokinetics of repetitive electrostatic pressurized intraperitoneal aerosol chemotherapy (ePIPAC-OX) as a palliative monotherapy for patients with isolated unresectable colorectal peritoneal PM (clinicaltrials.gov Identifier: NCT03246321).
- A non-randomized, non-blinded cohort study investigating the therapeutic effect of adjuvant PIPAC in resected high risk colon cancer patients (clinicaltrials.gov Identifier: NCT03280511).
- An open-label, single arm trial concerning the feasibility, efficacy and safety of PIPAC with oxaliplatin, cisplatin and doxorubicin in patients with PM from colorectal, ovarian, gastric cancer or with mesothelial primary (clinicaltrials.gov Identifier: NCT02604784).
- An open-label, single arm trial investigating the benefit of dose escalation of Oxaliplatin in PIPAC therapy for nonresectable peritoneal metastases of digestive cancers (clinicaltrials.gov Identifier: NCT03294252).
- An open-label, single arm, cohort study evaluating the efficacy of PIPAC against PM (clinicaltrials.gov Identifier: NCT03287375).

The present work aims at contributing to a deeper understanding of distribution and penetration depth of chemotherapeutic drugs, offered intraperitoneally as a pressurized aerosol during PIPAC therapy.

1.3.5 Limitations

Despite the above mentioned achievements, there are still limitations PIPAC technology is struggling to overcome. Applying standards regarding injection pressure, exposure time, availability, chemotherapeutic dose, injection angle, selection of chemotherapeutic drug and tolerable toxic side effects are still under intensive investigation and need to be evidenced to guaranteeing the best outcome.

First, the effect of pressure on the penetration depth still provides space for discussion. In an ex-vivo study, comparing different pressure levels and its impacts on penetration depth, increased pressure in the model box did not lead to a substantial higher penetration depth into the tissue (Khosrawipour et al., 2016b). Other studies reported a strong positive effect of increased intraperitoneal pressure on the drug uptake into tumoral tissue (Heldin et al., 2004, Minchinton and Tannock, 2006, Jacquet et al., 1996).

Second, the positioning of the Capnopen® has been shown to have a great impact on the target tissue in the spray jet, but not for the other peripheral samples. Yet, only a more homogenous distribution will effectively grant treatment conditions, no matter where exactly in the abdominal cavity the tumor nodules are located. To overcome this limitation, Khosrawipour et al have proposed various modifications for the application device. The Capnopen® could be placed at the most outlying position of the abdominal cavity. Furthermore, it could rotate during injection phase to ensure more equal distribution of the chemotherapeutic agent. Another idea would be to add several devices administering the aerosol from different directions(Khosrawipour et al., 2016b).

1.3.6 Side effects of chemotherapy

Systemic chemotherapy is the standard of care in patients with PM (Franko et al., 2016). There is a range of side effects, depending on the type of chemotherapeutic drug applied. Especially the fast dividing cell lines such as blood cells and the cells lining the mouth, the stomach and the intestines are affected. In general, toxicities related to the chemotherapy can occur in direct

temporal context (acute side effects) or develop chronically, between months and years.

Common acute side effects occurring after administration of chemotherapeutic drugs include nausea, vomiting, mucositis, diarrhea, paresthesia, cutaneous symptoms and alopecia (Odendahl et al., 2015). With regards of organ involvement, side effects typically include renal toxicity (cisplatin), neurotoxicity (oxaliplatin) and cardiac toxicity (doxorubicin) (Rossi et al., 2003, dos Santos et al., 2012, Carvalho et al., 2009). In general, systemic side effects occur less when chemotherapy is applied intraperitoneally (Emoto et al., 2012).

In PIPAC technology, cisplatin and doxorubicin are commonly administered with a tolerable locoregional toxicity. Only 10 % of the usual systemic drug dose is applied into the abdominal cavity. The systemic drug concentration is limited with 1 % of the systemic dose and 5 % of the HIPEC dose (Blanco et al., 2013).

In a pilot study, Blanco et al investigated the impact of PIPAC technology on renal and hepatic toxicities. Data obtained from three patients showed that PIPAC does not cause significant renal or hepatic toxicity. Laboratory values of gGT showed a slight increase in the first few postoperative days with a decrease afterwards; Bilirubin, Alkaline phosphatase and Quick did not change remarkably. Also, the serum creatinine levels stayed stable after application. No cumulative toxicity was observed after repeated applications of PIPAC (Blanco et al., 2013). In another trial with a larger patient cohort (14 patients, 40 PIPAC procedures, combined with systemic chemotherapy) no significant hepatic and renal toxicity was induced and no major postoperative complications (CTCAE ≥ 3) were observed (Robella et al., 2016).

In addition, different studies have shown that through establishing a positive intraabdominal pressure with a capnoperitoneum of 12 mmHg, both the portal and the renal blood flow impaired (Demyttenaere et al., 2007, Blanco et al., 2013, Schilling et al., 1997). An increase of the intraabdominal pressure by 5 mmHg leads to a significant blood flow decrease by 39% to the liver and 60% to the peritoneum. The longer the application time was, the less blood was transported through the splanchnic area (Schilling et al., 1997). These findings imply, that the

limited blood inflow into the abdominal organs during PIPAC application naturally leads to decreased outflow from the splanchnic circulation to the systemic compartment. This constellation favours both the bioavailability of the chemotherapeutic drug in the peritoneal tissue and a low systemic plasma concentration. As already mentioned above, the systemic drug concentration of doxorubicin is minimal, reaching about 1 % of the systemic dose and around 5 % of the HIPEC dose (Tempfer et al., 2018, Blanco et al., 2013).

1.4 Physical parameters

The following sections give insight into the physical parameters and central issues of PIPAC administration.

1.4.1 Aerosol

An aerosol is a heterogenous mixture of fine solid particles or liquid droplets and air or another gas. In nature, typical examples are fog, clouds, smoke, and soot. One must distinguish between monodisperse and polydisperse aerosols. Monodisperse aerosols contain particles of uniform size. However, most produced aerosols contain particles with a wide range of different particle diameters. In medicinal context, an aerosol is a drug containing substance, packaged under pressure with a gaseous propellant for release (Dictionary, Juli 2017). As a standard of care, aerosol sprays (containing cortisone, β_2 -adrenergic receptor agonists) are used in pulmonary medicine (Cazzola et al., 2012, Rubin, 2010).

The basic idea of using an aerosol for intraperitoneal chemotherapy is to take advantage of the physical properties of a gas, which expands homogenously within a closed space. In theory, the entire surface of the peritoneum can be reached by the drug-containing aerosol, which is one of the main advantages compared to conventional peritoneal lavage, where not all parts of the abdominal cavity are covered sufficiently. However, although an aerosol fulfils certain criteria to be regarded “gas-like”, one must keep in mind, that the generated aerosol also

contains droplets in the micrometer-size range, which clearly differ from the behavior of a perfect gas.

Scientific research on the droplet size distribution of the generated aerosol during PIPAC has presented a wide range of generated droplet sizes. Khosrawipour et al described that the Capnopen® sprays with a droplet diameter ranging from 3 – 15 μm (Khosrawipour et al., 2016a). In ex-vivo granulometric analysis by laser diffraction spectrometry, Göhler et al found out, that more than 92.5 number% of the released droplets have a diameter below 3 μm . Interestingly, considering the volume-weighted distribution, 97,5 vol% of the liquid is part of droplets with a diameter $\geq 3\mu\text{m}$. In other words, most of the volume of the released droplets turns up in a few larger droplets, whereas the majority of the droplets contains just a minimal fraction of the entire volume. Thus, most of the liquid volume is deposited either by inertial impaction or by gravitational settling. Only a small fraction of the liquid is carried by droplets in the sub-micrometer range diffuse in space like an ideal gas. Furthermore, two major peaks in the distribution curve of the generated droplets exist, beside one mode $< 3\mu\text{m}$, a second mode showed values between 10 and 15 μm (Gohler et al., 2017).

In the scientific community, there is still discussion about the appropriate droplet size diameter. The liquid particles of the aerosol behave the more “gas-like”, the smaller the diameter is. The equation of Stokes shows, that halving the diameter leads to a four times diminished sedimentation velocity (Britannica, April 11, 2016). Rubin et al announced, that if an aerosol is supposed to behave “gas-like”, the diameter should not exceed 1 μm (Rubin, 2010). However, one must keep in mind, that creating liquid droplets with a diameter $< 1\mu\text{m}$ is not only very difficult to achieve, it might also not even be necessary, since the therapeutic aerosol is even supposed to deposit after a certain time. Therefore, it is only important to approach to the characteristics of an ideal gas to guarantee sufficient homogenous distribution within the abdominal cavity.

An ideal gas will expand homogeneously within a closed space. Yet, an aerosol does not behave “gas-like”, i.e. distribute homogeneously within a closed space such as the abdominal cavity, but the liquid droplets of the aerosol will eventually

deposit due to different mechanisms. As mentioned above, through inertial impaction, larger particles deposit on the ground. Furthermore, gravitational forces lead to a sedimentation of smaller particles. This process is time depending, the smaller the particles, the slower the deposition.

In general, so far, there is just little knowledge about the mechanisms of aerosol therapy into the abdominal cavity. Much more information about the basic principles of aerosol therapy in pulmonary medicine is available. Aerosol therapy in pulmonary medicine is very demanding due to some major obstacles such as a needed patient compliance, a small anatomic diameter of the bronchial tubes, a complex geometry of the space of application (bronchial tree) and the impossible chemical and physical control.

Compared to that, abdominal aerosol application stands out for its low fragility of the application system, the absence of needed patient compliance, the large anatomic diameter, and the simple geometry of the abdominal cavity. Above all, the possibility of steering the environmental setting, as mentioned above, is regarded as a very important tool in effective tumoral treatment.

The creation process of an aerosol is based on two pathways: the technical devices and the drug-containing solution. In the available schematic overview, both pathways are considered equally important. The drug needs to have the required concentration in the solution. The angioinjector provides the upstream pressure, which is needed for the nebulizer to atomize the supplied solution and to spray it into the abdominal cavity. Only if all steps are coordinated accurately, the target effect on the tissue will fulfil the necessary requirements.

1.4.2 Distribution pattern

A homogenous distribution of chemotherapeutic agents within the abdominal cavity contributes considerably to an improved effectiveness of intraperitoneal tumor treatment. The abdominal cavity is subdivided into different regions (Solass et al., Pleura and Peritoneum 2017). As some parts of the abdominal cavity are very difficult to reach, intraperitoneal chemotherapy is not able to distribute homogeneously within the cavity, leaving poorly or untreated tumor tissue behind

(Khosrawipour et al., 2016a). Another aspect, that should be taken into concern is the fact, that administering a drug containing fluid into the abdominal cavity is also subject to the principles of gravitation forces. Thus, after administration and depending on time, the liquid is deposited in the deepest part of the abdominal cavity. Regions, situated under the abdominal wall, might not be reached adequately. Even more, after surgical intervention, patients often develop adhesions, which mark major obstacles in optimal drug distribution, because further PIPAC procedures might become impossible to perform (Nadiradze et al., 2016, Girshally et al., 2016).

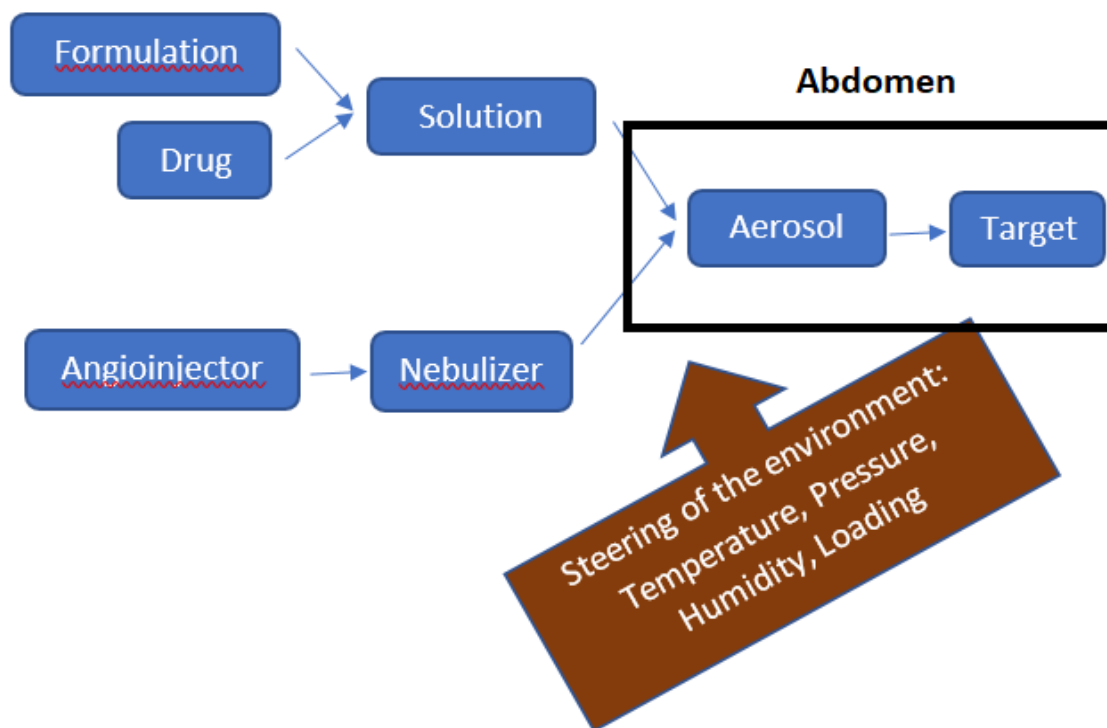


Figure 2: Quality by Design concept applied to the process of PIPAC procedure

Schematic overview of optimizing the therapeutic aerosol. Starting from the target effect onto the tissue, the aerosol is optimized by determined upstream parameters (device, solution) as well as by steering the intraabdominal environment (temperature, pressure, pH-value, charge).

1.4.3 Drug concentration

The drug concentration of the aerosolized solution in the abdominal cavity is very important for several reasons. As small peritoneal tumor nodules (<1mm) are

either poorly or not vascularized, intravenously administered chemotherapy does not reach its target, resulting in inefficient cytotoxic effects. For these nodules, a higher drug concentration is potentially advantageous. On the other hand, the currently used cytotoxic drugs are characterized through a steep dose-effect relationship, where a doubling of the dose will lead to multiplied toxic effects. (Ceelen and Flessner, 2010).

As currently standard of care, the concentration of doxorubicin and cisplatin in the atomized solution is determined with values of 10.5 mg/m² body surface (cisplatin) and 2.1 mg/m² (doxorubicin). These concentrations are supposed to ensure sufficient effectiveness in combating tumor cells combined with acceptable locoregional side effects (Blanco et al., 2013).

Recently, it was proposed that higher drug concentrations of Cisplatin/Doxorubicin were still well tolerated without major systemic toxicity. The maximum tolerable dose was not reached (Tempfer et al., 2018).

1.4.4 Hydrostatic pressure within the abdominal cavity

One must distinguish between the applied upstream pressure of the angioinjector and the elevated pressure while installing a capnoperitoneum. The drug is delivered via the angioinjector with an upstream of approximately 20 bars.

The elevated pressure in the abdominal cavity during PIPAC procedure has various consequences, such as increased intratumoral drug concentration (Jacquet et al., 1996), effective counteraction of the hydraulic capillary pressure (Minchinton and Tannock, 2006, Esquis et al., 2006) and a decreased drug outflow to the body compartment (Blanco et al., 2013, Schilling et al., 1997). Theoretically, the higher the intraabdominal pressure is set, the deeper the chemotherapeutic agents could possibly penetrate. The elevation of the intraabdominal pressure during laparoscopy is limited by hemodynamic and respiratory issues (Schilling et al., 1997). Therefore, in clinical practice, the current limit of intraabdominal pressure during HIPEC is 10 – 15 mmHg (Garofalo et al., 2006); for PIPAC applications, 12 mmHg is the standard of treatment (Nowacki et al., 2018).

1.4.5 Depth of drug tissue penetration

The penetration depth is an important marker to analyze the efficacy of chemotherapeutic therapy. The deeper a cytotoxic agent can infiltrate into tumoral tissue, the more tumor cells are killed.

Theoretically, a high penetration depth can be achieved by applying a positive pressure in the abdominal cavity (pneumoperitoneum). Thus, the therapeutic drug containing aerosol will penetrate deeper inevitably due to physical laws. Additionally, the homogenous drug distribution pattern also plays a role, which should not be underestimated. As described later in detail in the chapter “discussion”, effective penetration into peritoneal tissue only happens in regions of the cavity, where the aerosol has been propagated and stayed during the exposure period of PIPAC application.

In conventional lavage of the abdominal cavity, reported penetration depth results are variable ranging from a few cell layers (for Doxorubicin and Mitoxantrone), 2 mm (for Mitomycin C and Oxaliplatin)(Ceelen and Flessner, 2010) up to 3-5mm (for cisplatin)(van de Vaart et al., 1998) with a mean tissue concentration of 0.03 $\mu\text{mol/g}$ (Jacquet et al., 1996). Compared to that, PIPAC shows a chemotherapeutic penetration depth both into tumoral and peritoneal tissue reported at 300 – 600 μm and parallel to that a significantly higher tissue concentration (up to 4.1 $\mu\text{mol/g}$) (Solass et al., 2014).

1.5 Scientific problem

One of the central issues in PIPAC research is the achievement of homogeneity of drug distribution within the abdominal cavity. In the scientific community, there is consent about the fact, that a homogenous drug distribution is a precondition for approaching the long-term goal of treating PM with a curative approach.

In the past, many efforts have been made to describe and improve the distribution pattern of an aerosol. Different models including in vivo, ex vivo and postmortem swine experiments have dealt with the relation between the injected aerosol, the distribution pattern within the abdominal cavity and the penetration depth into the

serosal tissue. Yet, homogeneity in drug distribution could not yet be achieved in a satisfactory manner. All presented models suffer from different limitations. In order to move scientific research of the PIPAC technology forward, it has become essential to develop new preclinical models.

In this context, a new ex vivo experimental model, the inverted bovine urinary bladder, is introduced as one key element of this dissertation. Detailed information about the experimental set up and the advantages of this model will be given in the following chapters.

In all established models, measurements only recorded the result of application, as defined by serosal staining, tissue concentration or penetration depth. This is a significant restriction, since aerosol distribution is not static, but time-dependent. Thus, in the present work, the Thermographic Imaging, an established method in other contexts, is introduced as another new dynamic experimental model, analyzing the injection behavior and the consecutive spatial distribution of the aerosol over time in a closed space.

This dissertation puts its focus on the description and improvement of the aerosol distribution pattern. In doing so, in the following chapters, the physical properties of two aerosols, created by two different nebulizers, the Capnopen® and a prototype device (in the following called Prototype4), will be analyzed in various series of experiments. The objective of these experiments is to gain a deeper understanding of the drug distribution pattern of aerosols with improved characteristics and their effects on the penetration depth and drug concentration in the serosal tissue.

2 Methods

2.1 Ethical and regulatory framework

This study involved no human patients and no human tissue, therefore no approval by the Ethics committee of the University of Tübingen was needed. Fresh biological tissue was obtained from the slaughterhouse from animals sacrificed for the alimentary chain. No living animal was used or sacrificed for the purpose of this study, therefore no application to the local Animal welfare committee was required.

2.2 Study design

This is an experimental study using in-vitro and ex-vivo models for comparing the performance of two medical devices: the CE-certified Capnopen® (Capnomed GmbH, Villingendorf, Germany) vs. a second-generation instrument (“Prototype 4”), provided by the same company. This research was performed under the umbrella of a contract research agreement between Capnomed GmbH and University of Tübingen. The study was fully funded by Capnomed GmbH.

Results were documented according to the good scientific practice standards of the German Research Foundation (DFG) and comply with the “Empfehlungen zur Führung eines Forschungs-Protokollbuches” of the Faculty of Medicine, University of Tübingen (Version 12/2017). Experimental records were uploaded on the LabGuru platform of the research group (AG PIPAC).

For being able to evaluate the medical devices, it was first necessary to develop adequate models, since such models were not available. Since it would appear unethical to perform a large number of experiments in animals, we first developed two preclinical models: a Thermographic Imaging in-vitro model and an ex-vivo model using biological tissue: the inverted bovine urinary bladder model.

2.3 In-vitro models

In a first step, we measured the granulometric characteristics of the aerosol depending on the medical device design. For this purpose, we used an established, FDA-approved method for analyzing medical aerosols.

In a second step, we evaluated homogeneity of aerosol distribution depending on the device. For this purpose, we proposed, developed and implemented a new model to visualize spray propagation by Thermographic Imaging.

2.3.1 Granulometric analysis

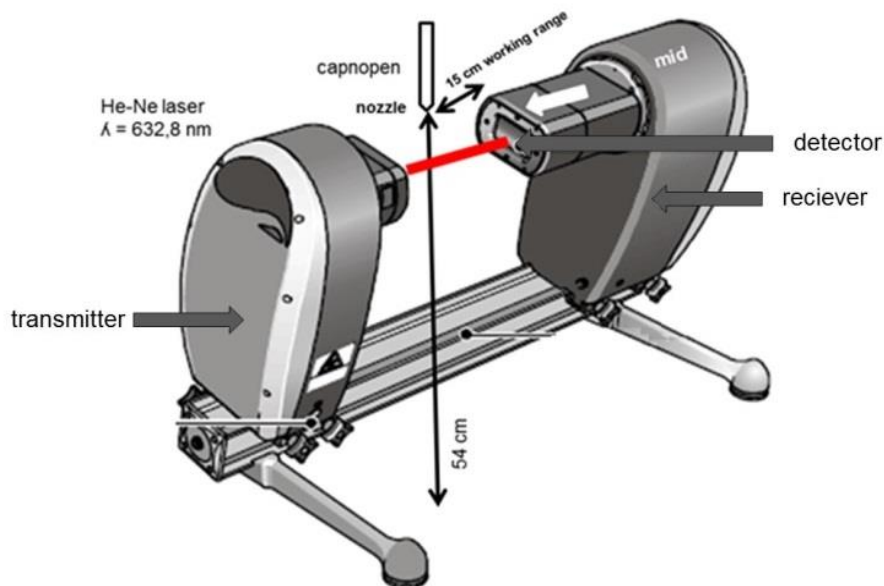


Figure 3: Experimental setup of the SprayTec® droplet analyzer

Droplet size distribution analyses were performed by laser diffraction with the SprayTec® droplet analyzer (Malvern Instruments, Worcestershire, UK).

The helium-neon laser, located in the transmitter, emits a 10-mm light beam (wavelength: 632,8mm). Through the aerosol droplets, the laser light is scattered and recorded via the silicon-diodes detector array (detection rate: 1 Hz) in the receiver. The distraction of the laser light is transformed into the droplet size distribution by means of defined mathematic algorithms (Fraunhofer theory). The

SprayTec® droplet analyzer can detect droplet diameter within a range of 0.1 – 2000 µm. Measurements were taken for the Capnopen® and the Prototype4.

The nebulizer was positioned in a perpendicular position 5 cm above the center of the open laser beam. Flowrate was 1 ml/min, 120 ml aqua was aerosolized and recording time was 2 min.

2.3.2 Thermographic Imaging

The idea of our newly developed Thermographic Imaging model was to create a closed gaseous environment with dimensions comparable to a human abdomen, and to generate a therapeutic aerosol within the closed volume with a warming screening placed beyond the aerosol. The hypothesis was the colder aerosol would “hide” the warm screen, allowing therefore to determine aerosol distribution in real time by thermographic recording. The experimental setup for Thermographic Imaging consists of a radiated surface, which is heated up to 100 °C. In front of the surface, a cupola box with a plain ground and an arc-type roof is built. The ground and the upper wall consist of hard plastic plates. The measures of the experimental box are: height 14 cm, width 35 cm and depth 22 cm. The front of the box is sealed by commercially available plastic wrap.

In the center of the roof, a hole with a diameter of 15 mm is drilled, through which the Capnopen® is inserted in a perpendicular position, hereby the tip of the noddle goes 5 mm into the box.

Thermography is an imaging method for displaying the surface temperature of objects. The intensity of the infrared radiation is interpreted as a measure of its temperature. A thermal imaging camera converts the infrared radiation, which is invisible to the human eye, into electrical signals, which are converted into a colored image.

The thermographic camera (Seek Thermal®) is positioned 40 cm in front of the box and connected to a commercially available smartphone where the images are captured. Thus, the lens of the camera is situated at about 1 cm above an imaginational horizontal line, which passes the bottom of the box in the center.

Prior to the aerosol injection, the camera captures the uniform temperature distribution of 100 °C. After the aerosol injection into the box chamber, the temperature distribution changes, since the aerosol reduces the infrared radiation. The camera takes one picture every second, thus the dynamics of the spray propagation can be observed.

In the experiments, both the Capnopen® and the Prototype4 were used under identical circumstances.

Table 1: Injection parameters for Thermographic Imaging

Aerosol	Duration	Flow rate	Temperature of radiator
aqua	30 secs	0.5 ml/sec	100 °C

Results were obtained by visual examination and analysis of the thermographic images.

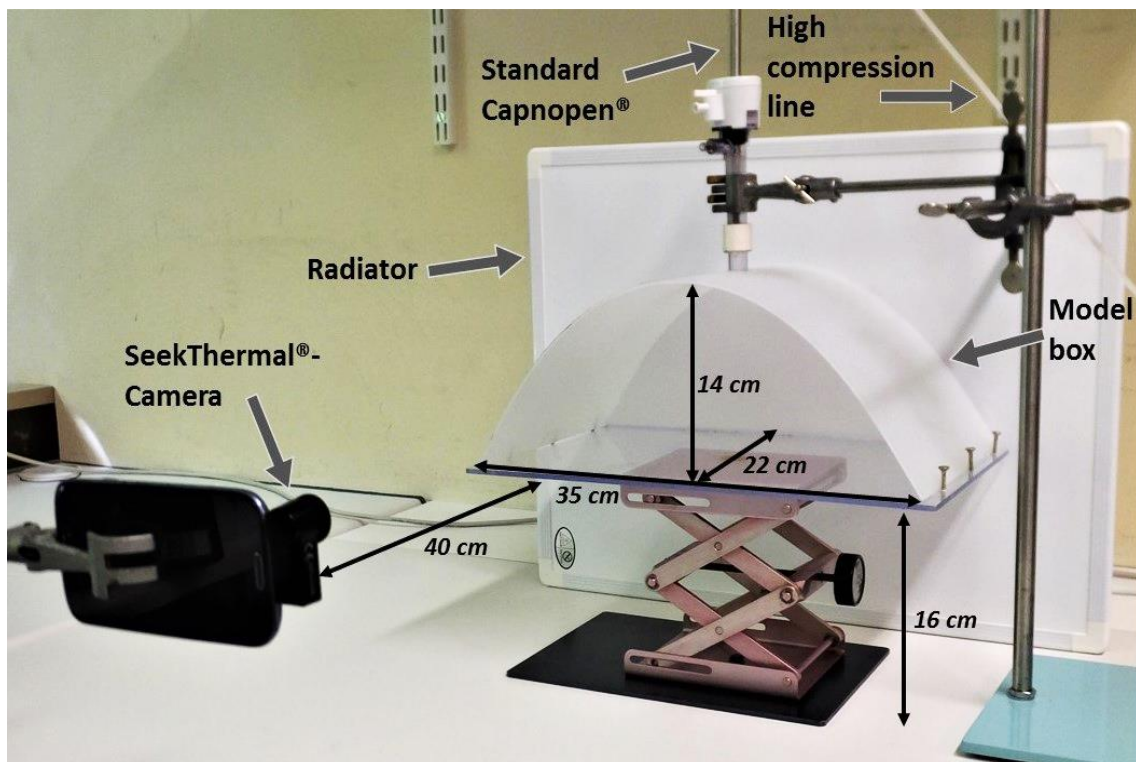


Figure 4: Experimental setup of Thermographic Imaging experiments

2.4 Ex-vivo models

The in-vitro models described above do not allow indeed to draw any conclusion on the effect of the therapeutic aerosol on the target tissue. Only through further development of the physiochemical properties of a therapeutic aerosol, drug delivery into the target cells can be optimized. For example, Khosrawipour et al. has demonstrated recently that the homogeneity of the therapeutic aerosol applied during PIPAC is not perfect. However, the experimental model used by these authors (tissue fragments placed into a plastic container box) was suboptimal because the plastic surfaces are not absorbing any substances so that the aerosols droplets are falling down rapidly to the floor of the container, due to gravity. For such a purpose, it was necessary to develop an additional, new model including serosal tissue. The model should be easy to use, reproducible and cost-effective. It should have a volume similar to the human abdominal cavity, and an oval shape. The inner surface should be lined with serosa. The model should allow pharmacological and biological analysis, including histology. No living animals should be used (Schnelle et al., 2017).

2.4.1 Inverted bovine urinary bladder

The volume of the bovine urinary bladder (2-3 l) compares well with the volume of the human abdominal cavity (3-5 l). By inverting the urinary bladder, the serosal surface, which normally marks the outside of the organ, becomes the inner surface. This setting allows adequate evaluation of both drug distribution and the drug penetration depth into the serosal tissue. Importantly, the serosal surface is homogeneous, which would not be the case in an animal model where anatomical and physiological characteristics of the peritoneum differ between various locations. For example, small bowel serosa – which permits bacterial translocation – might be much more permeable to macromolecules than the gastric serosa. Thus, evaluation of the influence of technical factors on homogeneity of aerosol distribution in vivo might be biased by organ-specific factors (Schnelle et al 2017). Purpose of our first experiments was to investigate the feasibility of the model as well as its functionality.

2.4.2 Medical devices

The experimental equipment included following components:

- a high pressure angioinjector (Accutron HP, Medtron, Saarbrücken, Germany),
- a nebulizer (Capnopen® or Prototype4, Capnomed, Villingendorf, Germany)
- a CO₂-insufflator (Aesculap® AG, Tuttlingen, Germany)
- a 12 mm trocar (Kii®, Applied Medical, Düsseldorf, Germany)
- the inverted bovine urinary bladder
- various connecting lines.

Technical procedure

All organs were obtained cooled directly from the slaughterhouse. Then, each bovine urinary bladder was adequately dissected and rinsed with a physiological solution. The bladder was incised at the neck with a 4-cm cut and then inverted. Afterwards, a 12-mm trocar was inserted through the neck and adequately fixed by closing the organ with a purse-string suture. After installing a constant capnoperitoneum of 12 mmHg in the inverted bovine urinary bladder, various solutions (Methylene blue, ICG, DAPI and Cisplatin) were aerosolized into the inverted bladder with a flow rate of 0.5 ml/sec. After the exposure phase (15/30 min), the respective aerosol was evacuated over a closed system into HEPA filters and the bladder was disconnected from the apparatus. Then, the bladder was opened via a vertical cut from the neck to the bottom. Later experimental steps were depending on the kind of experiment (see below).

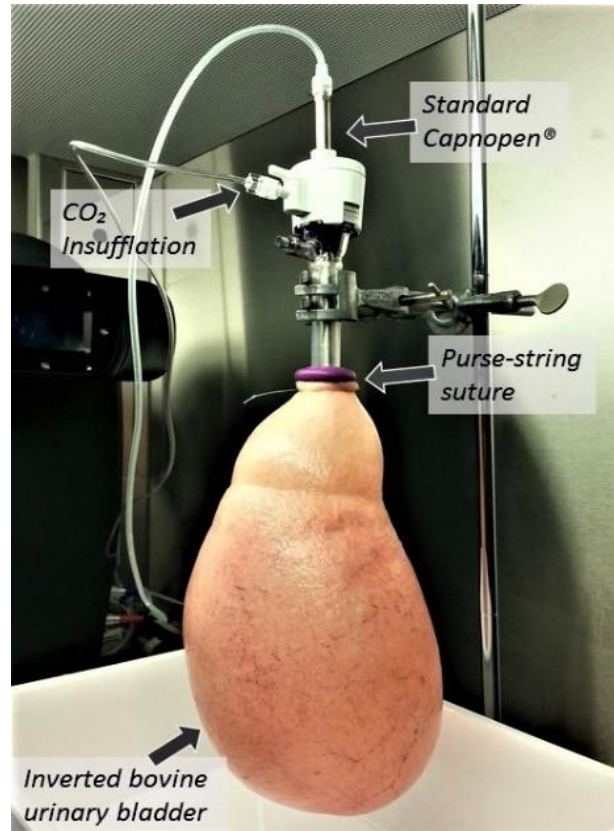


Figure 5: Experimental setup of inverted bovine urinary bladder experiments

Comparison of two nebulizers

The functional principle of the nebulizer is to generate an aerosol out of a liquid substance, which is injected under pressure into the experimental model. In the experiments, two different devices were tested. The Capnopen®, which is currently used in the operative setting of PIPAC procedures and a prototype (Prototype4).



Figure 6: Medical devices: Capnopen® and Prototype4

High pressure injector

The Accutron HP-D (Medtron®AG, Saarbrücken, Germany), a commercial high-compression injector, was used to compress the solution with an upstream pressure of 40 bar. It was connected to the nebulizer via a high compression infusion line.

As current operational standard of PIPAC, the injection flow rate in our experiments was 0,5 ml/sec. Depending on the amount of the drug-containing solution, the injection time varied.

CO₂ – Insufflator

The CO₂-Insufflator (Aesculap® AG, Tuttlingen, Germany) receives the CO₂ from a connected CO₂ bottle. In the beginning of each experiment, the CO₂-Insufflator was tightly connected via a connecting tube to the trocar, which was positioned in the neck of the bladder. Then, a constant positive pressure of 12 mmHg was established within the inverted bovine urinary bladder.

Aerosol

In all experiments, an aerosol was generated through the nebulizer (Capnopen®/Prototype4). Differences in the aerosols came from various solution formulations.

Table 2: Solution formulations of inverted bovine urinary bladder experiments

Experiment	Solute	Solvent	Ratio	Volume	Duration of injection
1	Methylene blue	0.9% NaCl	0.0003%	30 ml	60 secs
2	DAPI	0.9% NaCl	1 µg/ml	100 ml	200 secs
	ICG		10 µg/ml		200 secs
3	Cisplatin	0.9% NaCl	7.5 mg/m ² body surface	150 ml	300 secs

Sample Removal

After exposure phase, the bladder was taken off from the apparatus, opened via a vertical cut and positioned and presented for sample removal. Standardized 8 mm punch biopsies were taken in the experiments with DAPI and Cisplatin.

In the distribution experiment with DAPI, six samples were removed from predefined areas (in each case two from the upper, middle and bottom part).

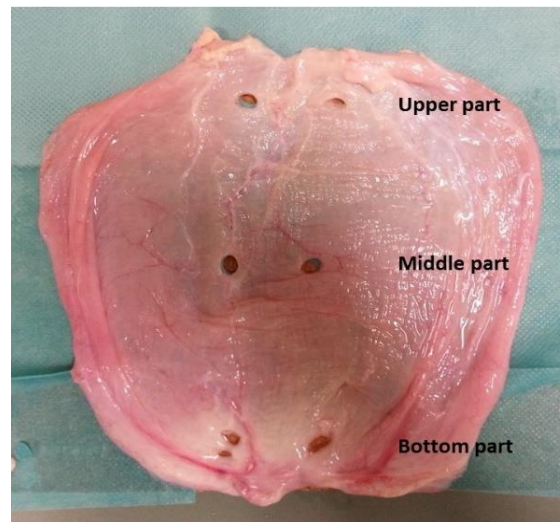


Figure 7: Interior view of a sliced inverted bovine urinary bladder after sample removal

In the distribution experiment with Cisplatin, nine samples were removed from predefined areas (in each case three from the upper, middle and bottom part).

Documentation of the tissue samples included date, number of bladder, area of sample removal and applied nebulizer (Capnopen® or Prototype4). After removal, samples were immediately frozen at -80°C for histological preparation.

2.4.3 Distribution experiments with Methylene Blue (visual examination)

For photodocumentation, opened bladders were positioned with the neck of the bladder upside. In total, three experiments were performed with Capnopen®, one with Prototype4. Homogeneity of the distribution pattern was investigated qualitatively by visual examination.

2.4.4 Distribution experiments with ICG (macroscopy) and DAPI (microscopy)

A combined solution consisting of Indocyanine green (ICG) and 4',6-diamidino-2-phenylindole (DAPI) was created according to the parameters of table 3.

With each device (Capnopen® and Prototype4), four series of experiments were performed.

ICG as a dye is used frequently for medical diagnostic purposes such as visualizing liver metastases and retinal blood circulation (Handgraaf et al., 2017, Guerrero et al., 2017). The absorption maximum light wavelength is about 750 to 800 nm (Alander et al., 2012). The emitted fluorescence spectrum of ICG is very wide, varying between 750 nm and 950nm (Sabapathy V, 2015).

DAPI is a fluorescence dye, which is commonly used in fluorescence microscopy for marking DNA. The absorption maximum light wavelength is 358 nm, the emission maximum 461 nm. During fluorescence microscopy, DAPI is excited through ultraviolet light and detected using a cyan filter (Kapuscinski, 1995).

Formulation of the solutes-containing solution was as follows:

Table 3: Aerosol formulation and application parameters of ICG/DAPI experiments

Solute	Solvent	Volume	Ratio	Injection Rate	Duration of Injection
DAPI	0.9% NaCl	100 ml	1 µg/ml	0.5 ml/sec	200 secs
ICG			10 µg/ml		

After the exposure time of 30 min, the inverted bovine urinary bladder was opened and positioned on a cork plate for photodocumentation of ICG. Afterwards, tissue samples were taken to analyze penetration depth of DAPI.

Photodocumentation of ICG (macroscopy)

For photodocumentation, a completely darkened room was used. The opened bladder was positioned under the IC-View Camera (Pulsion Medical Systems AG, D-München). Excited ICG (wavelength 780 nm) in the bladder wall was detected and photo-documented with the IC-View Camera. Of each bladder, one image was taken. Homogeneity of the ICG distribution pattern was investigated qualitatively by visual examination.



Figure 8: IC-View Camera

The digital video camera (Sony®, Digital 8 Video Camera Recorder DCR-TRV820E) is connected with a fluorescence emission device (Pulsion Medical Systems AG, D-München, wavelength 780 nm), which creates the excitation of ICG in the bladder wall

Fluorescence Analysis of DAPI (microscopy)

A fluorescence microscope (DM-RBE 55453®, Leica Systems, Leipzig, Germany) was used for DAPI penetration depth measurements. Excitation wavelength of DAPI is 358 nm. A filter only lets pass the DAPI fluorescence light (emission maximum of 461 nm). The microscope was coupled to the image-editing program LeicaQWin (Leica Microsystems Imaging Solutions Ltd, Cambridge, UK), with which penetration depth measurements in the serosal tissue were performed.

From each bladder, six tissue samples were taken, out of which three histological cuts each were created. The technically best prepared histological cut was selected. Out of it, three representative sections of the serosal surface were

evaluated with three penetration depth measurements each (experiment in triplicate). In total, 54 measurements for each bladder were documented.

Evaluation of tissue penetration depth was performed by an independent pathologist, who was blinded to the type of device used and to the position of the sample in the bladder.

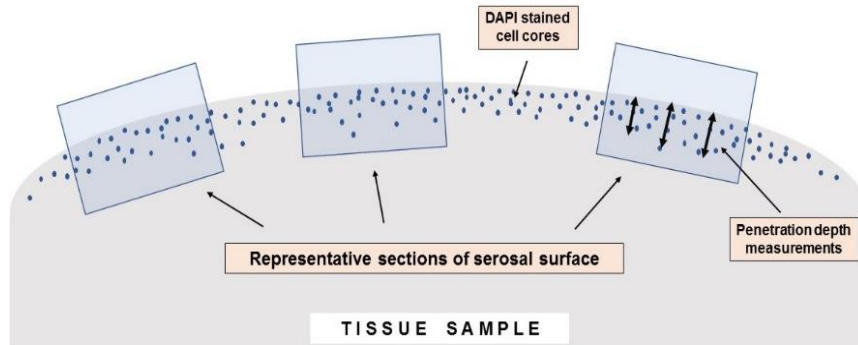


Figure 10: Schematic selection of three representative sections in a tissue sample

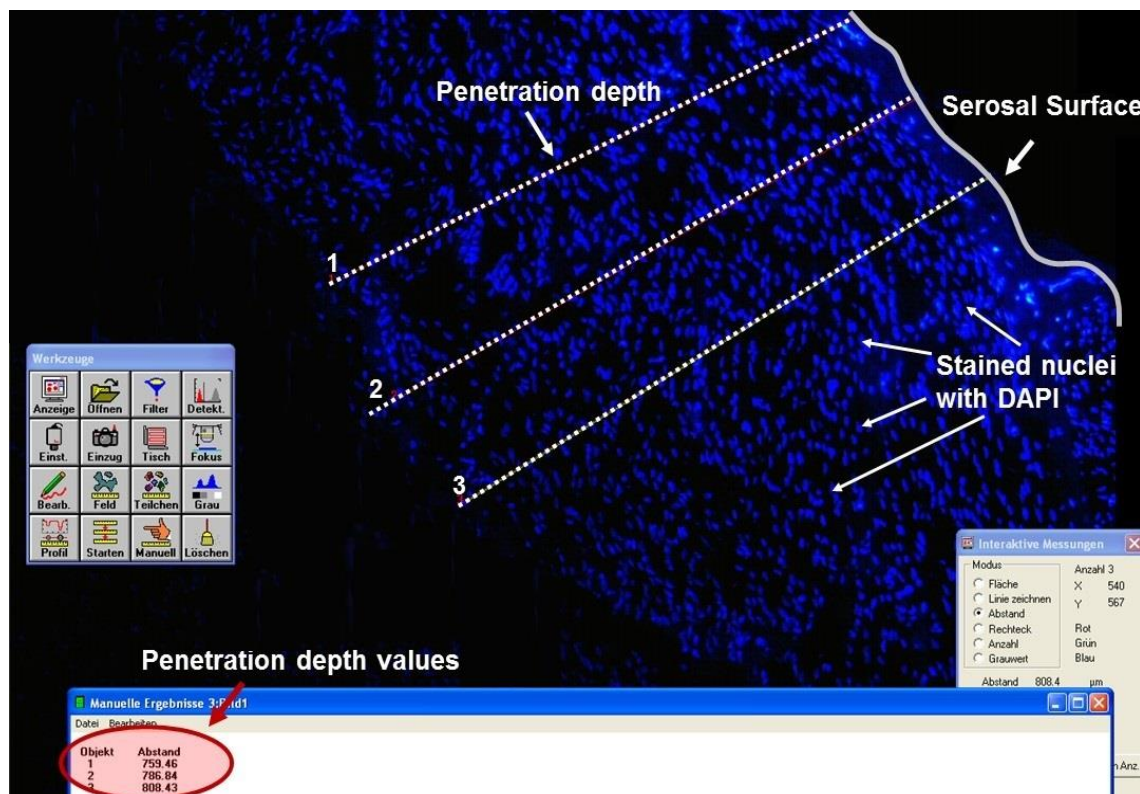


Figure 10: Exemplary image of penetration depth measurements with fluorescence microscopy

The white dotted lines indicate the three performed penetration depth measurements. See the serosal surface in the upright corner and the DAPI stained nuclei (blue). 10x Enlargement.

2.4.5 Distribution experiments with Cisplatin (tissue concentration)

Chemotherapy experiments were conducted in order to assess the drug concentration in the tissue samples in predefined areas within the bladder. Therefore, Cisplatin was disposed with the same setup. Just Capnopen® was tested. Three series of experiments were performed.

Formulation of the drug containing solution was as follows:

Table 4: Aerosol formulation and application parameters of Cisplatin experiments

Drug	Solvent	Volume	Ratio	Injection rate	Duration of Injection
Cisplatin	0.9% NaCl	150 ml	7.5 mg/m ² body surface	0.5 ml/sec	300 secs

The Cisplatin-containing solution was injected for 300 secs, with an injection rate of 0.5 ml/sec. Exposure time was 30 min.

Out of each bladder, nine tissue samples were taken, frozen at -80°C for subsequent histological preparation and analysis.

Histological preparation and concentration analysis

Frozen tissue samples were lyophilized (KF-2-110; H. Saur Laborbedarf, Reutlingen, Germany) in the a vacuum concentrator and weighted. The pellet was cut into 3 - 4 little pieces, followed by resuspension in 1 ml Ampuwa water. Samples were homogenized with a micra-D9 homogenizer (ART-moderne Labortechnik e.V) for 1 min and then sonicated in a sonicator (Electrosonic type 07 or ELMA S30/H) for 20 min at room temperature. Afterwards, samples were shaken in an overhead rotator overnight at room temperature (Roto-Mix, Typ ROTO, neoLab, Germany). Samples are filled up with 1,0 ml Ampuwa (distilled water) to give a final volume of 2,0 ml followed by vortexing, centrifugation and aservation at -80°C until shipping.

Finally, samples were shipped on dry ice to the laboratory "Überörtliche Berufsausübungsgemeinschaft, Medizinisches Versorgungszentrum, Dr.

Eberhard & Partner” in Dortmund, where concentration measurements of cisplatin with atomic absorbance spectroscopy (AAS) were conducted.

2.5 Occupational health safety aspects

For research purpose, toxic aerosols were generated and manipulated during this study. The experiments were performed within a class-2 safety hood certified for application of cytostatic drugs (Maxisafe 2000, ThermoFisher Scientific, Dreieich, Germany). All related procedures have been audited by the safety officer of University Hospital Tübingen and by the competent health insurance (Unfallkasse Baden-Württemberg) in Q4/2016. Environmental air measurements were performed according to a standard protocol (NIOSH 7300) by an independent company (DEKRA industrials, Stuttgart, Germany). No traces of platin were detected with a detection limit of 0.3 ng/m³ (Schnelle et al., 2017).

2.6 Statistics

Since this is exploratory research, no size sample was determined a priori. All experiments were performed in triplicate. Blinding was applied when possible, in particular for analysis of depth of tissue penetration. Descriptive analyses of the data included mean \pm CI 95%, or median and percentiles. The data were graphically presented as box plots. Comparative statistics included non-parametric tests for comparison of means. The statistical program SPSS Version 22.0. (IBM Corp. Released 2013. IBM SPSS Statistics for Windows, Armonk, NY: IBM Corp.). Probability values were defined as follows: were performed and the accompanying diagrams created. *p < 0,05; **p < 0,01; ***p < 0.001; and ‡p > 0.05.

3 Results

3.1 Granulometric analysis

In this chapter, the results of the droplet size distribution analysis by Laser Diffraction are presented.

The diagram in figure 11 shows the particle diameter distribution of Capnopen® (black) and Prototype4 (red) in a logarithmic scale. The y-axis indicates the volume frequency in percent. The values of droplet diameter distribution are volume-weighted. The curve of Prototype4 ascends steeper, has its peak with over 30 % volume frequency at the particle diameter of 34 µm (compared to 24% using Capnopen®), and again falls down faster compared to the curve of Capnopen®.

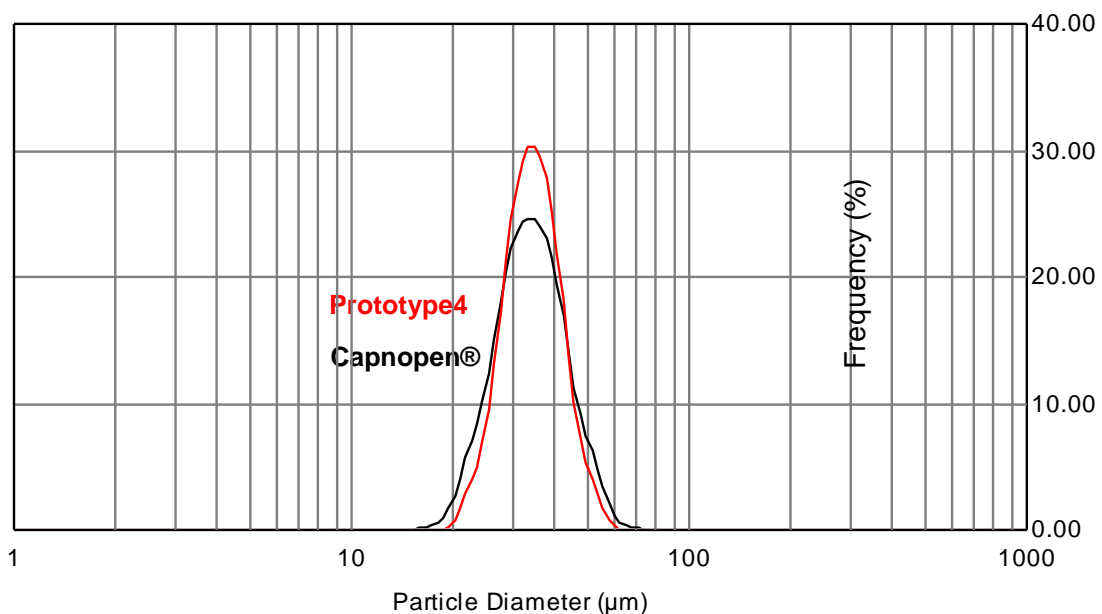


Figure 11: Particle diameter distribution of Capnopen® and Prototype4

Table 5: Comparison of different diameter values ($D_v(10)$, $D_v(50)$, $D_v(90)$)

	$D_v(10)$	$D_v(50)$	$D_v(90)$
Capnopen®	24.82 µm	33.81 µm	45.72 µm
Prototype4	26.82 µm	34.24 µm	43.64 µm

Values are indicated in micrometers

Table 5 compares three different diameter values of both Capnopen®. The value $D_v(50)$ indicates the median particle size. 50% of the droplets are below this value. Other important parameters are $D_v(10)$ and $D_v(90)$, which determine the range of the majority of the droplet sizes. The diameter of 80% of the droplets is in between these two values. The smaller the difference between $D_v(90)$ and $D_v(10)$, the more droplet size homogeneity within the aerosol exists.

The $D_v(50)$ of the Prototype4 is slightly higher than of the Capnopen®. The Prototype4 has a lower $D_v(90)$ and a higher $D_v(10)$ than the Capnopen®. That indicates that the Prototype4 has a more uniform spray pattern with a smaller range of droplet size distribution compared to the Capnopen®.

3.2 Thermographic Imaging

3.2.1 Results of Thermographic Imaging

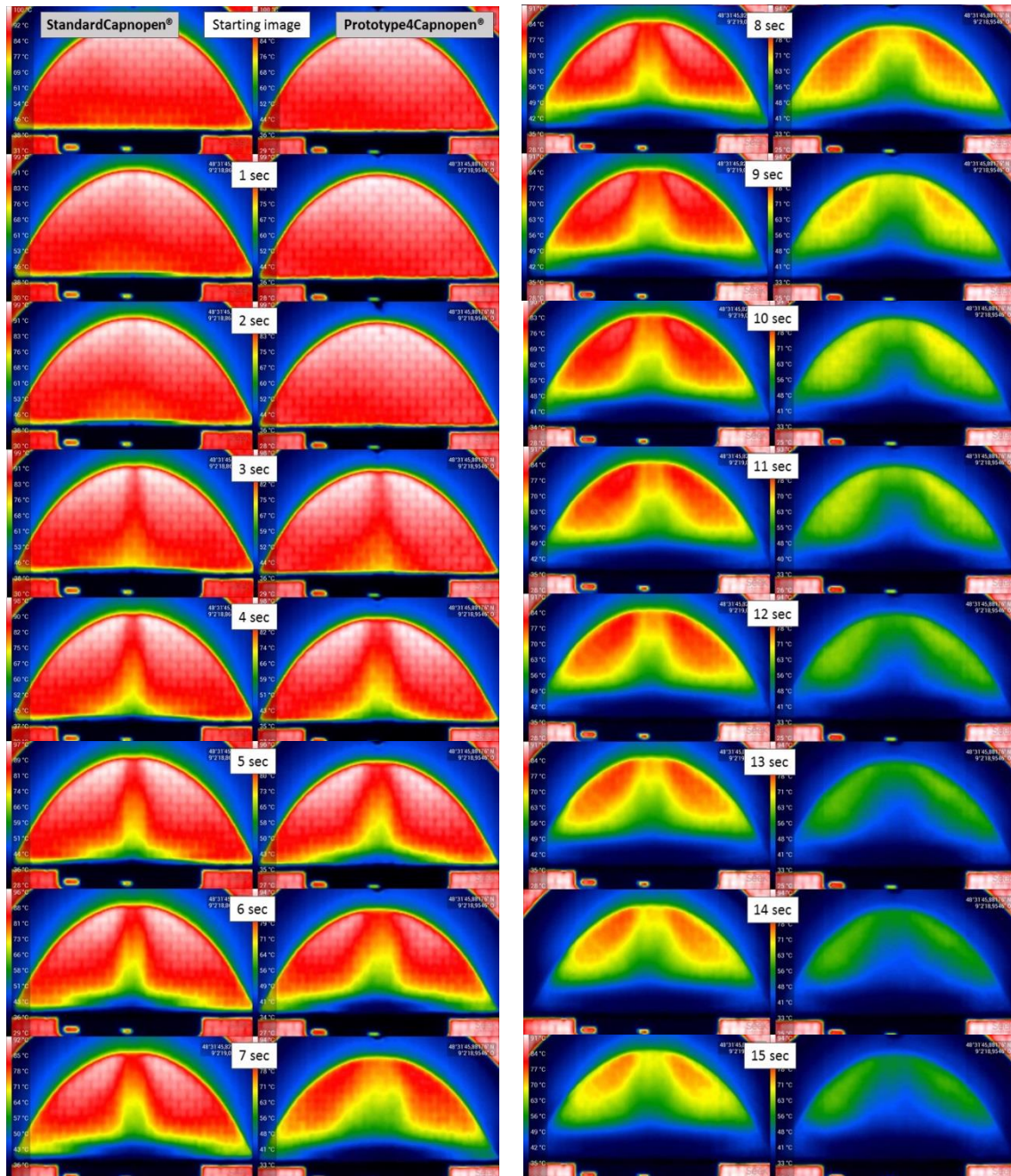
The basic idea of Thermographic Imaging is to make infrared radiation, emitted by all bodies with a temperature level above absolute zero, visible. The amount of radiation, emitted by an object, increases with rising temperature. Thermographic cameras operate in the long-infrared range of the electromagnetic spectrum (approximately 9 – 14 μm). The received electromagnetic waves are transformed into an image with different temperature levels.

Thermographic Imaging is a valid possibility to describe the spatial distribution of an aerosol injected into a model box over time. Here, this technique makes use of the fact that the appearance of an aerosol leads to decreased heat transmission. The more droplets of the aerosol are injected in a certain space, the less heat of the radiator, which is located behind the model box, can be transmitted, leading to a decreased temperature. This direct connection between number of droplets in space and decreased heat transmission is interpreted in the experiments. Two different nebulizer (Capnopen® and Prototype4) were used in the experiments.

Temperature levels are defined as follows:

Table 6: Temperature levels of Thermographic Imaging

Red area	Yellow area	Green area	Blue area
77 – 84 °C	66 – 72 °C	53 – 61 °C	< 49 °C



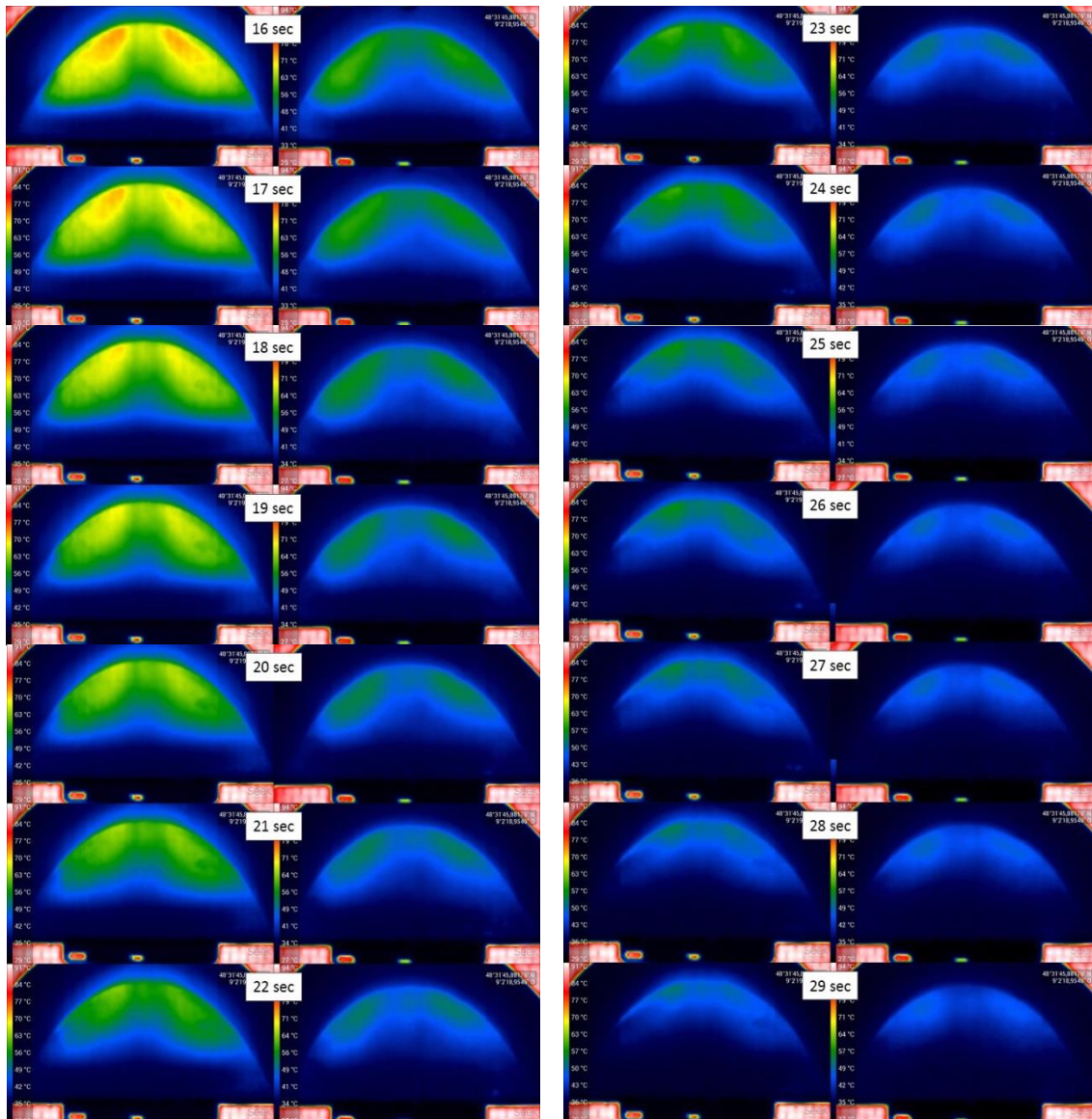


Figure 12: Thermographic Imaging during injection period into model box

Emitted infra-red radiation from a radiator, placed behind the box, is received by the Seek Thermal® camera and converted into thermograms. A series of 30 subsequent image pairs is shown, which were captured every second. The left images display the temperature pattern for Capnopen®, the right images for Prototype4.

3.2.2 Description of the thermographic images

Capnopen® - Images left column

The starting image marks the beginning of injection. After 1 sec, a dark spot has appeared on the ground of the model box. After 3 secs, first signs of spatial cooling are visible in the center of the model box. A symmetrical tent-like

darkening, starting mainly on the ground at first and then raising and widening the more aerosol is injected. Additionally, the ground area changes color from at the beginning yellow to green to blue, the more time passes. After 7 seconds, a respectable amount of aerosol droplets covers the entire ground.

Another phenomenon can be observed from the image after 11 seconds. On the sides of the model box, cooling proceeds faster than in the space between the sides and the center. This can be explained by the flow behavior of the aerosol, which is injected into the center, then spreads out to the sides and finally soars up again.

After 18 seconds, the red areas have finally disappeared, having changed into yellow and green sections. The “w”-shaped line, marking the upper end of the concentrated aerosol distribution, gradually moves upwards, until after 29 seconds, just two small dark green spots beside the central injection spot are left.

Prototype4 - Images right column

After starting the aerosol injection, images of both Capnopen® are comparable until 4 secs. Afterwards, in the right images, the central cupola grows faster with a larger diameter. The biggest contrast between the images of both Capnopen® can be observed after 10 secs. While with the Capnopen® the upper area is still red except for the already cooled down ground and the central aerosol flow path, with Capnopen® 2, the red parts in the upper center have already disappeared and the blue sections reach the center of the model box.

The central conical elevation of the cooled area has a larger diameter. This characteristic of the Prototype4 can be best observed after 9 secs.

Within six seconds (between image after 4 secs and after 10 secs), the entire volume of the model box is filled with aerosol droplets. From this point, further cooling of the side upper areas proceeds steadily and homogeneously, until after 29 secs, a cooling of all areas in the model box has occurred.

3.2.3 Comparison of properties of Capnopen® and Prototype4

The injection angle of Capnopen® is $\alpha = 40^\circ$, while Prototype4 offers an angle of $\beta = 55^\circ$.

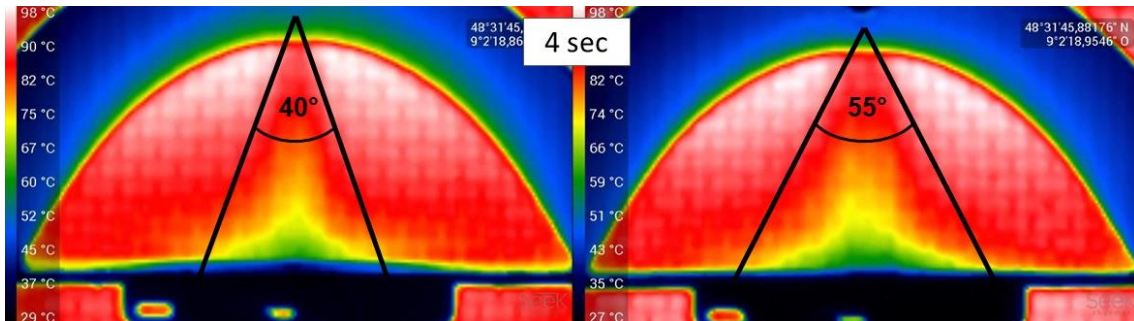


Figure 13: Injection angles of Capnopen® (left) and Prototype4 (right)

In addition, the distribution velocity of both devices differs significantly.

Table 7: Comparable aerosol distribution snapshots

Capnopen®	Prototype4
5 secs	4 secs
10 secs	7 secs
19 secs	10 secs
29 secs	25 secs

Table no. 7 shows comparable snapshots of the respective intermediate distribution results. The spreading degree of the aerosol of Prototype4 after 4 secs corresponds to the spreading degree of the aerosol of Capnopen® after 5 secs. The aerosol distribution velocity of Prototype4 is higher. Especially noticeably is the almost doubled time between the image of Prototype4 after 10 secs and the image of Capnopen® after 19 secs.

3.3 Inverted bovine urinary bladder experiments

In this chapter, the results of the three inverted bovine urinary bladder experiments are presented.

3.3.1 Distribution experiments with Methylene Blue (visual examination)

Staining of the entire serosal surface except the upper part of the bladder neck, which was unreachable for the aerosol due to the tight pursuing suture, was revealed both in the approaches with Capnopen® and Prototype4. Although the upper half of the bladder was dyed properly, most intense staining was observed in the lower parts.

No substantial difference in the homogeneity of surface staining between the Capnopen® and the Prototype4 was observed.

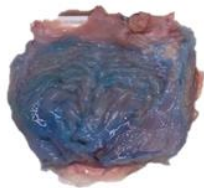
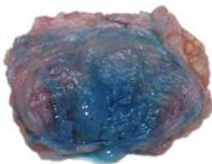
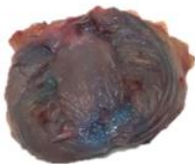
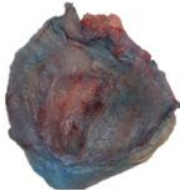
Test	# 1	# 2	# 3	# 4
0.9% NaCl				
Pen Generation	Capnopen®			Prototype4

Figure 14: Overview of the stained bovine urinary bladders after opening

Bladders #1 - #3 were treated with Capnopen®, bladder #4 with Prototype4. Staining of all bladders was performed with Methylene Blue

3.3.2 Distribution experiments with ICG (macroscopy)

The images 1 – 4 document the four urinary bladders being sprayed with Capnopen®. Prototype4 was used in the bladders 5 – 8.

Description of Fluorescence Imaging with Capnopen®

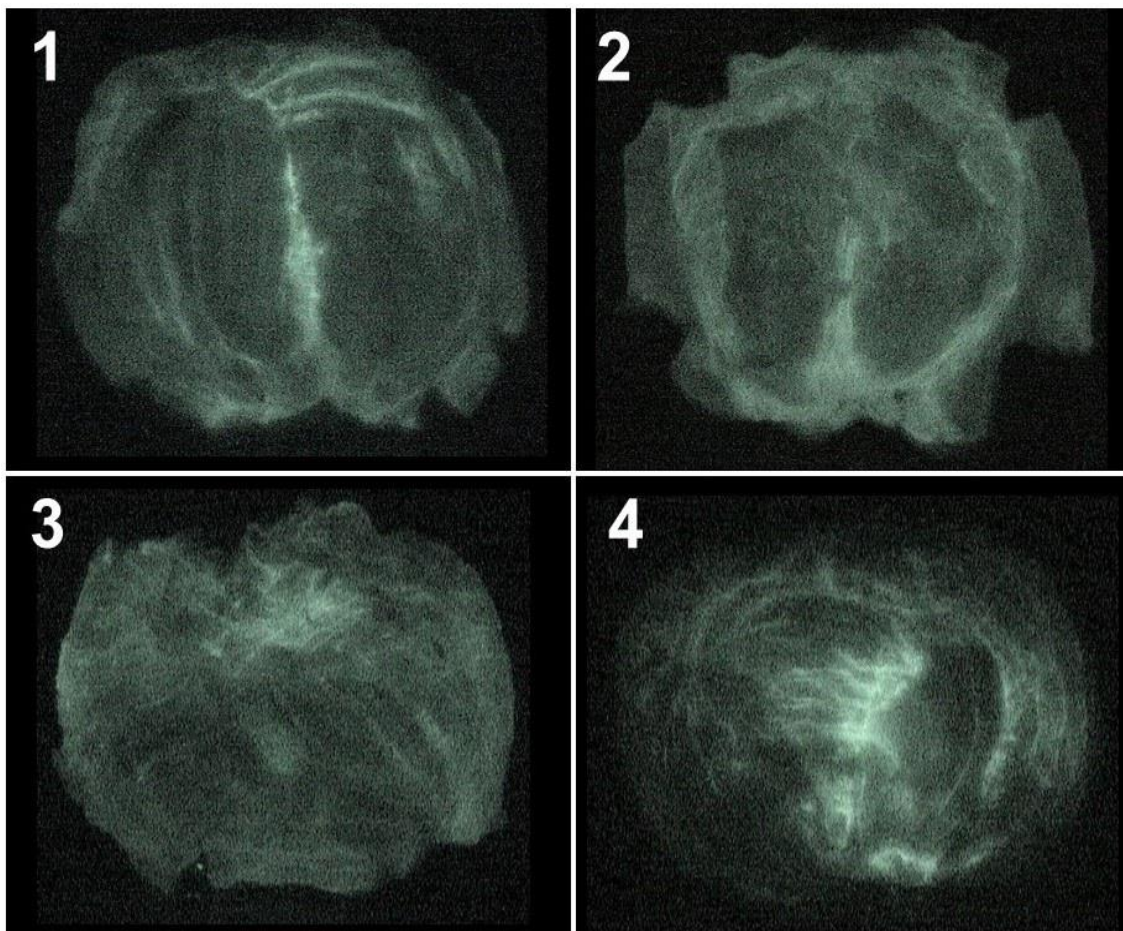


Figure 15: Photo documentation of ICG-sprinkled bladders with the Capnopen®

In the images 1 – 4, the bladders sprayed with Capnopen® are shown. The upper part indicates the neck of the bladder. In all four bladders, ICG fluorescence emission is apparent.

Table 8: Characteristics of ICG aerosolized bladders (Capnopen®)

	Characteristics
Bladder no° 1	Image shows a homogeneous distribution of ICG in all parts of the bladder with emphasis on the center and connective tissue bands. In the upper parts emitted fluorescence is as strong as in the lower parts.
Bladder no° 2	Image shows a considerable homogeneous distribution of ICG in all parts of the bladder with emphasis on the bottom and connective tissue bands. In the upper parts emitted fluorescence seems stronger than in the center, strongest parts in the bottom.
Bladder no° 3	Image shows a homogeneous distribution of ICG in all parts of the bladder with emphasis on the upper parts and connective tissue bands. The margins of the bladder are clearly definable.
Bladder no° 4	Image shows a heterogeneous distribution of ICG in the bladder. Especially in the center of the bladder, ICG fluoresces quite strong. The upper parts are rather omitted as well as the left side.

With Capnopen®, the distribution of the emitted fluorescence light is reasonably uniform with focus on certain areas within the bladder. The lines with higher brightness levels, which run through the bladder, correlate with fibrous connective tissue. This becomes apparent especially in the image of bladder no° 4. No essential difference in the brightness level between the upper and the lower parts of the bladders can be observed.

Description of Fluorescence Imaging with Prototype4

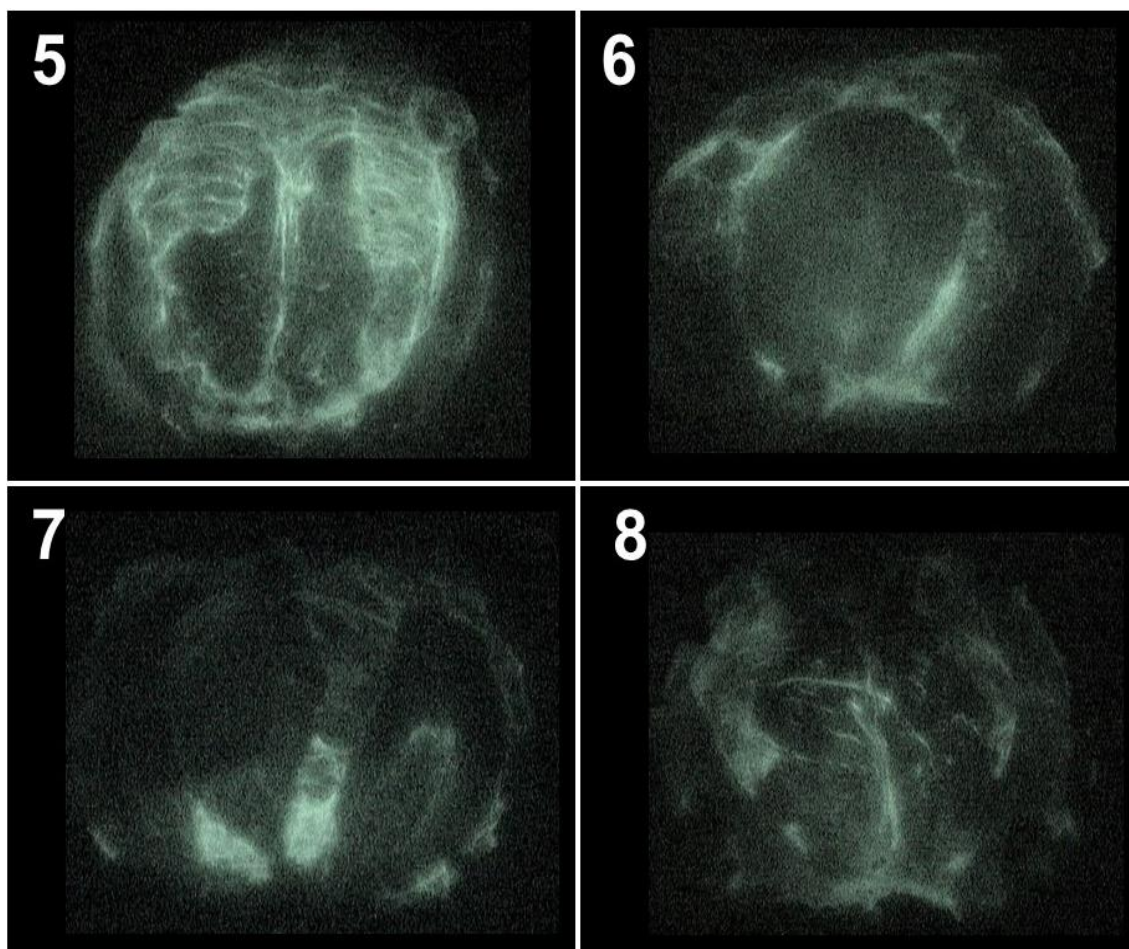


Figure 16: Photo documentation of ICG-sprinkled bladders with the Prototype4

In the images 5 – 8, the bladders sprayed with the Prototype4 are shown. The upper part indicates the neck of the bladder. In all four bladders, ICG fluorescence emission is apparent.

Table 9: Characteristics of ICG aerosolized bladders (Prototype4)

	Characteristics
Bladder no° 5	In general, signal level is very high. All edges of the bladder are clearly definable. Image shows a considerable homogeneous distribution of ICG in all parts of the bladder with emphasis on the upper parts and connective tissue bands.
Bladder no° 6	In general, signal level is moderate. Clearly definable edges on the left side, vague edges on the right side. Image shows a considerable homogeneous distribution of ICG in all parts of the bladder with emphasis on the lower parts and connective tissue bands.
Bladder no° 7	Signal level differs from intense (lower parts) to weak (upper parts). Edges of the bladder are not always clearly definable. Image shows a significantly higher fluorescence in the lower parts. As a straightly drawn and sharp border between the different signal levels is visible, there might have occurred some technical problems with the IC-View Camera.
Bladder no° 8	In general, recorded fluorescence power is satisfactory. Edges of the bladder are not always clearly definable. Image shows a spotted distribution of ICG in all parts of the bladder with emphasis on the lower parts.

Comparison between Capnopen® and Prototype4

Common ground in the experiments of both nebulizers is the emission of fluorescence light in all parts of the respective bladders. There are no parts within the bladder without any accumulation of ICG.

However, differences exist regarding the signal intensity level. In the images of the Capnopen®, the distribution pattern of the fluorescent ICG is very homogenous with similar signal intensity levels. Compared to that, in the images of Prototype4, signal intensity levels vary from intense (bladder no. 5), modest (bladder no. 6) to low (bladders no. 7&8).

3.3.3 Distribution experiments with DAPI (microscopy)

For each of both Capnopen® generations, penetration depth measurements in three regions (top, middle, low) of the bladders were performed, using fluorescence microscopy in order to detect the DAPI stained cell cores. The ideal objective of 54 measurements for each region (3 bladders x 2 tissue samples x 3 images x 3 measurements) was achieved once (Prototype4/Low). In the other cases, between 21 (Capnopen®/Low) and 48 (Prototype4/Middle) were performed. Reasons for missing measurements were difficulties in histological preparation, which did not allow precise measurements.

In the following sections, first the results for the Capnopen® are presented and second the results for the Prototype4 followed by a comparison. All following diagrams and table are divided into three columns, which represent the top, the middle and the low part of each bladder.

Penetration depths with Capnopen®

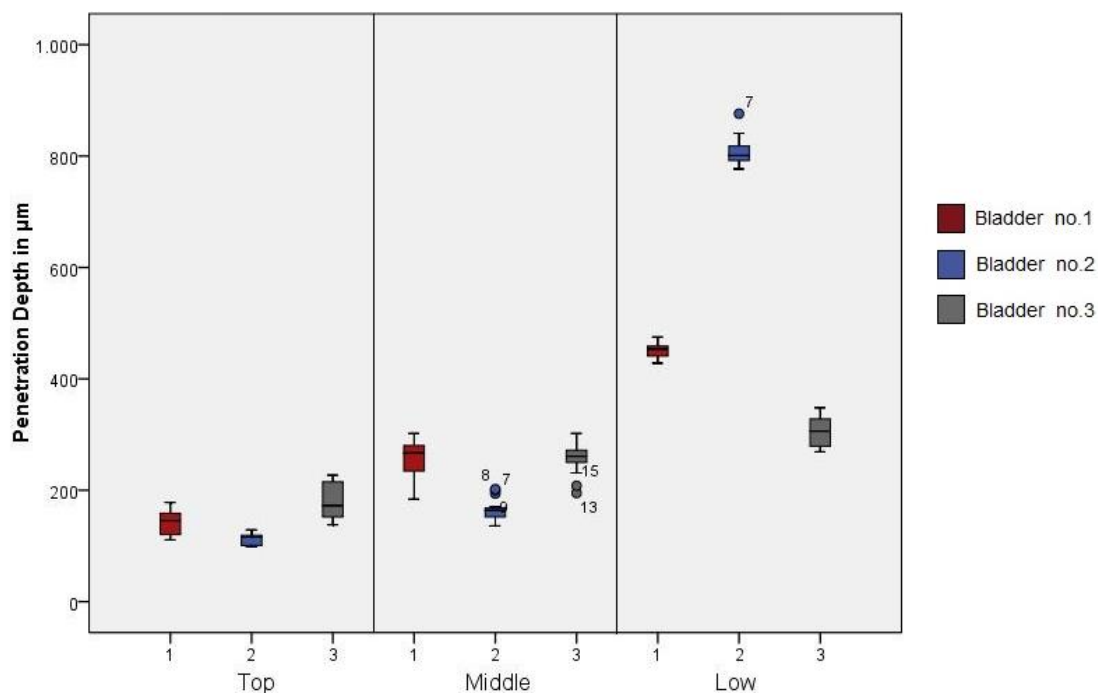


Figure 17: Graphic representation of different penetration depths depending on the position in the bladder (Capnopen®)

The x-axis indicates the regions of measurement within the bladder (top/middle/low). Y-axis indicates the penetration depth in micrometer.

Bladder no. 1 (red) shows an increasing penetration depth with **144 µm** (mean)(n=12; median 146; max 178; min 111; stand dev 23) on top, **257 µm** (mean)(n=15; median 267; max 302; min 184; stand dev 37) in the middle and **452 µm** (mean)(n=6; median 454; max 475; min 428; stand dev 16) in the low region.

Bladder no. 2 (blue) shows an increasing penetration depth with **113 µm** (mean)(n=9; median 116; max 129; min 98; stand dev 11) on top, **164 µm** (mean)(n=15; median 164; max 202; min 136; stand dev 20) in the middle and **812 µm** (mean)(n=9; median 801; max 876; min 777; stand dev 30) in the low region.

Bladder no. 3 (grey) shows an increasing penetration depth with **179 µm** (mean)(n=18; median 173; max 227; min 138; stand dev 33) on top, **257 µm** (mean)(n=15; median 261; max 302; min 195; stand dev 29) in the middle and **306 µm** (mean)(n=6; median 306; max 348; min 269; stand dev 30) in the low region.

Table 10: Summary of penetration depth results (Capnopen®)

	Top	Middle	Low
No. of bladders	3	3	3
No. of measurements	39	45	21
Minimum	98	136	269
Maximum	227	302	876
Mean	153	226	564
Median	151	243	459
Standard deviation	37	53	228
25 Percentile	119	168	338
50 Percentile	151	243	459
75 Percentile	175	268	798

Values (minimum – 75 percentile) are indicated in micrometers

The penetration depth values are always highest in the low part of the bladders. This is valid for all relevant statistical parameters such as mean, median, minimum, and maximum. However, the related standard deviation is relatively

high. Lowest penetration depth is observed in the top part of the bladders. The difference between top and middle part is relatively low, whereas the difference between middle and low part is much higher.

Penetration depths with Prototype4

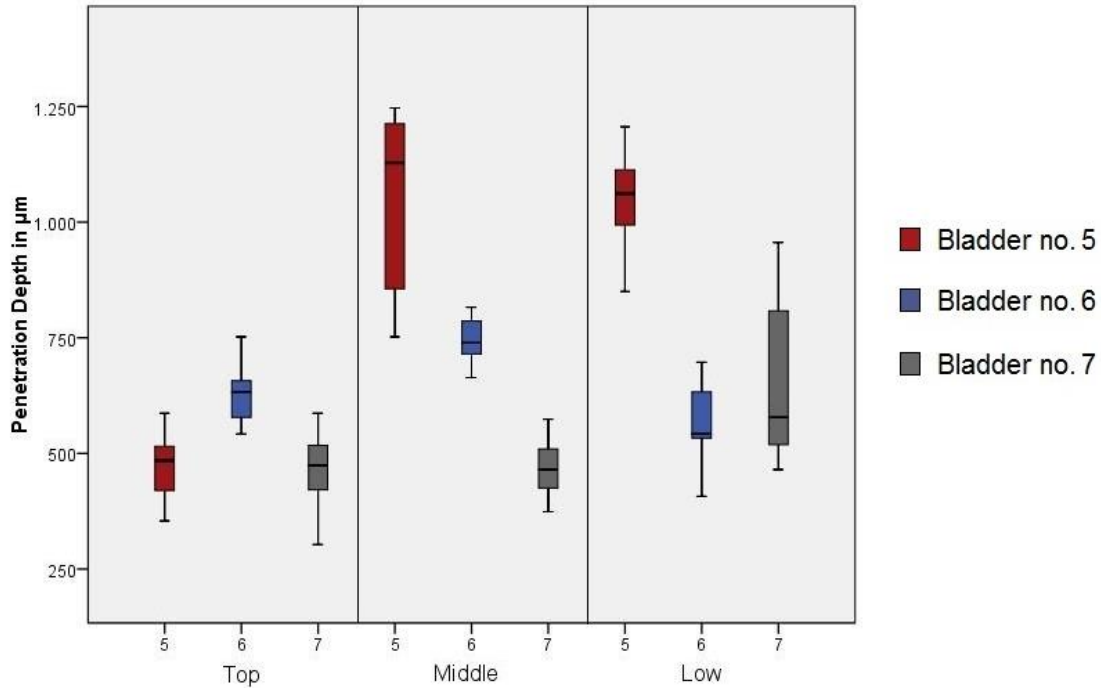


Figure 18: Graphic representation of different penetration depths depending on the position in the bladder (Prototype4)

The x-axis indicates the regions of measurement within the bladder (top/middle/low). Y-axis indicates the penetration depth in micrometer.

Bladder no. 5 (red) shows an increasing penetration depth with **473 µm** (mean)(n=18; median 485; max 587; min 354; stand dev 63) on top, **1128 µm** (mean)(n=18; median 1129; max 1247; min 752; stand dev 188) in the middle and **1045 µm** (mean)(n=18; median 1062; max 1206; min 850; stand dev 850) in the low region.

Bladder no. 6 (blue) shows an penetration depth distribution with **633 µm** (mean)(n=9; median 633; max 752; min 542; stand dev 71) on top, **746 µm** (mean)(n=18; median 740; max 816; min 664; stand dev 45) in the middle and **561 µm** (mean)(n=18; median 543; max 697; min 407; stand dev 78) in the low region.

Bladder no. 7 (grey) shows an increasing penetration depth with **465 μm** (mean)(n=15; median 474; max 587; min 303; stand dev 83) on top, **470 μm** (mean)(n=12; median 465; max 587; min 374; stand dev 62) in the middle and **646 μm** (mean)(n=18; median 579; max 956; min 465; stand dev 166) in the low region.

Table 11: Summary of penetration depth results (Prototype4)

	Top	Middle	Low
Measurements	42	48	54
Minimum	303	374	407
Maximum	752	1247	1206
Mean	504	791	750
Median	511	755	644
Standard deviation	98	259	244
25 Percentile	436	597	537
50 Percentile	511	755	644
75 Percentile	558	959	244

Values (minimum – 75 percentile) are indicated in micrometers

Comparing the data, certain statements can be made: The minimum increases from 303 μm on top to 374 μm in the middle and 407 μm in the low region. The maximum also increases in the beginning from 752 μm to 1247 μm and the slightly diminishes to 1206 μm in the low region. Both the mean and the median have their maximum value of 791 μm (755 respectively) in the middle, followed by 750 μm (644 respectively) in the low region. The lowest mean (respectively median) can be found on top. The highest standard deviation of 259 μm can be observed in the middle, followed by the low part and the top.

Comparison between Capnopen® and Prototype4

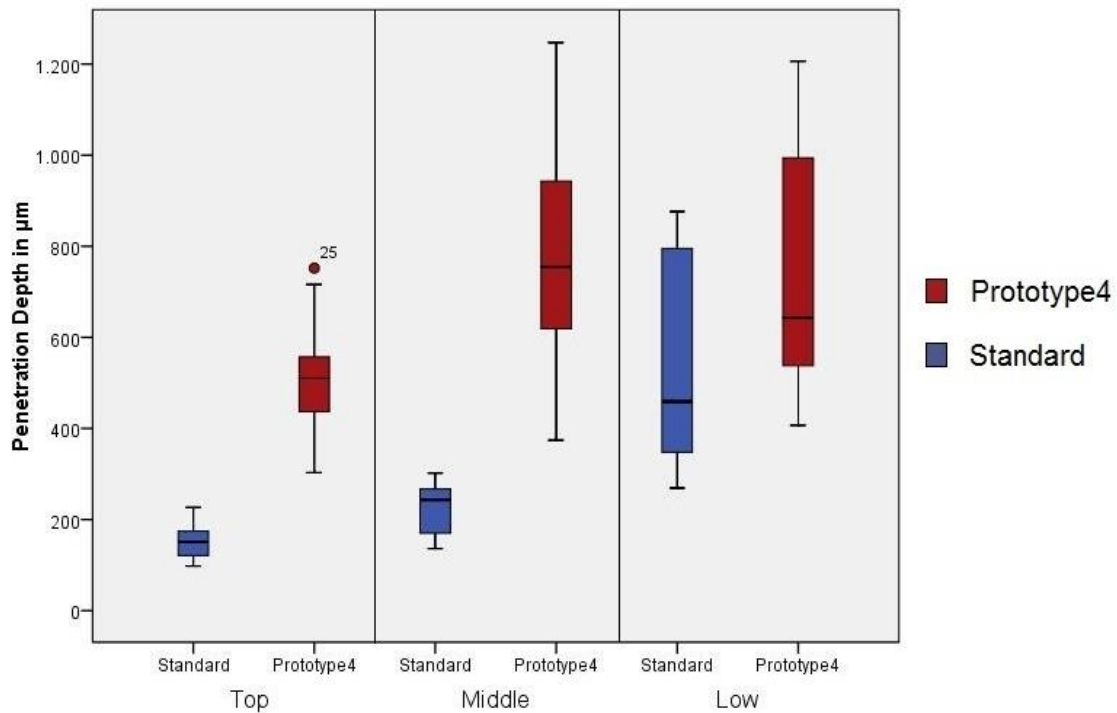


Figure 20: Penetration depths of Capnopen®/Prototype4 sorted by regions

The different penetration depths into inverted bladder serosal tissue after aerosolizing with the Capnopen® (identified by the blue box plots) and the Prototype4 (red box plots) are shown. X-axis indicates the regions of measurement within the bladder. Y-axis indicates the penetration depth in micrometer.

The penetration depths of Prototype4 are clearly above those of the Capnopen® regardless of the investigated area.

The most substantial difference between the two pens is observed in the middle region of the bladder. There, the Prototype4 achieves penetration depth values comparable to those in the low region. In comparison, the Capnopen® shows a highly different penetration depth for the middle and low region.

The standard deviation in general is much higher for the Prototype4 compared with the Capnopen®, especially in the middle region.

3.3.4 Distribution experiments with Cisplatin (tissue concentration)

In three experiments, 27 tissue concentration measurements in three regions (9 top, 9 middle, 9 low) of the bladders.

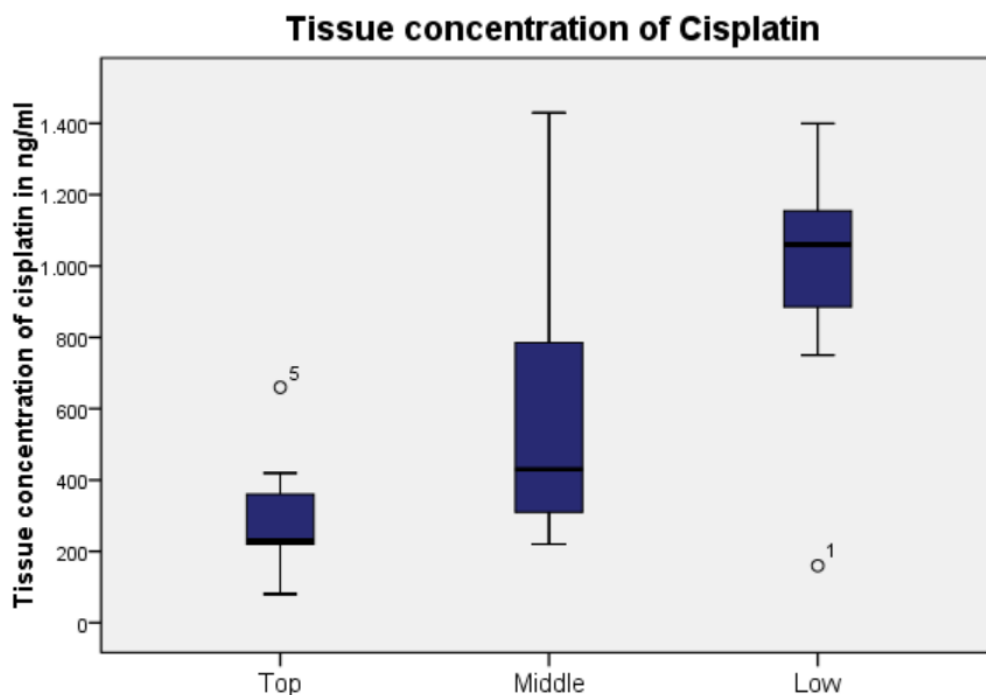


Figure 21: Tissue concentration of Cisplatin sorted by regions (Capnopen®)

The x-axis indicates the regions of measurement within the bladder (top/middle/low). Y-axis indicates the tissue concentration in nanogram per milliliter.

Table 12: Summary of tissue concentration results

	Top	Middle	Low
Measurements	9	9	9
Minimum	80	200	160
Maximum	660	1430	1400
Mean	295	580	968
Median	230	430	1060
Standard deviation	171	398	356
25 Percentile	188	300	817
50 Percentile	230	430	1060
75 Percentile	390	855	1173

Values (minimum – 75 percentile) are indicated in nanograms per milliliter.

The table shows a mean tissue concentration of cisplatin with **295 ng/ml** (mean)(n=9; median 230; max 660; min 80; stand dev 171) on top, **580 ng/ml** (mean)(n=9; median 430; max 1430; min 200; stand dev 398) in the middle and **968 ng/ml** (mean)(n=9; median 430; max 140; min 160; stand dev 356) in the low region.

Comparing the data, certain statements can be made: The minimum increases from 80 μm on top to 200 μm in the middle and diminishes to 160 μm in the low region. The maximum also increases in the beginning from 660 μm to 1430 μm and then slightly diminishes to 1400 μm in the low region. Both the mean and the median have their maximum value of 968 μm (1060 respectively) in the low part, followed by 580 μm (430 respectively) in the low region. The lowest mean (respectively median) can be found on top. The highest standard deviation of 259 μm can be observed in the middle, followed by the low part and the top.

4 Discussion

In this chapter, the results for the central scientific questions are presented. First, the new inverted bovine urinary bladder model is discussed. Second, the new investigation methods for the transient aerosol formation and spray propagation during the injection phase are discussed. This is followed by the discussion of the aerosol distribution pattern and tissue penetration depth achieved for the two tested nebulizer (Capnopen® and Prototype4).

4.1 Development and validations of preclinical models

4.1.1 Inverted bovine bladder model: characteristics and advantages over existing preclinical models

For further technical development of the PIPAC technology, preclinical models are needed to investigate and improve the physico-chemical characteristics of the injected aerosol. The advantages and disadvantages of experimental approaches for the optimization of the pressurized aerosol including the new inverted bovine urinary bladder model have been recently published (Schnelle et al., 2017).

Up to now, experimental investigation of the distribution pattern of an aerosol has been performed in various models. These PIPAC models included studies ex vivo (Solass et al., 2012a, Khosrawipour et al., 2016a, Khosrawipour et al., 2016b), in vivo (Solass et al., 2012b) and postmortem (Khosrawipour et al., 2016c). Yet, these experimental models suffered from either technical or anatomical limitations. For example, the in-vivo swine model (Solass et al., 2012a) had a lack of easy reproducibility and handling and was expensive. The plastic container model (Khosrawipour et al., 2016a) did not match the requirements of a model, which mimics the characteristics of the abdominal cavity. The droplets of the aerosol deposited on the plastic walls of the model and then drained down to the bottom of the box due to gravitational forces and lack of absorption. This inadequacy can be avoided by the walls of the bovine organ, which are able to absorb the applied aerosol.

The requirements for an experimental model, which comes very close to the properties of the abdominal cavity, are multiform. For example, the model should be lined completely with serosa, have an oval shape, and contain a volume similar to the abdominal cavity. Furthermore, it should be easy in handling, reproducible and the cost-effective. Additionally, it should allow pharmacological and histological analysis. All these parameters apply for the inverted bovine urinary bladder.

The inverted bovine urinary bladder is a new ex-vivo model, in which the physico-chemical properties of the injected aerosol can be investigated and improved effectively.

The following main effects can be evaluated by the inverted bovine bladder model:

- Penetration depth and drug concentration of the therapeutic aerosol within the serosal tissue and the possibility of histological sampling. As inversion of the urinary bladder can be achieved very easily (through a small incision in the bladder neck, the bladder can be inverted), this ex vivo model offers the opportunity of evaluating the target effect of a therapeutic substance onto the mucosa (normal, not inverted state) and the serosa (inverted state).
- Homogeneity of aerosol distribution via various experiments: Staining of serosa with methylene blue and ICG Fluorescence Imaging.
- Differences in the effects of various therapeutic substances (DAPI, methylene blue, ICG, Cisplatin, Doxorubicin): pharmacodynamic studies can be carried out with the inverted bovine urinary bladder
- Optimization of the physico-chemical parameters of the operating environment: influence of pressure, temperature and electrostatic charges.

Table 13: Characteristics of different experimental approaches for pressurized aerosol optimization

	In-vivo large animal model	Tissue fragments in a plastic container	Ex-vivo inverted bovine urinary bladder
Living animal needed	✓	x	x
Costs	High	Low	Low
Role of anatomical factors and vascularization	Considered	Not considered	Not considered
Adequacy of the parietal surfaces	Excellent	Poor	Good
Handling	Cumbersome	Moderately easy	Easy
Reproducibility	Moderate	High	High
Evaluation of technical factors	Difficult	Easy	Easy

Overview of advantages and disadvantages of different experimental approaches for pressurized aerosol optimization (Schnelle et al., 2017).

The ex-vivo inverted bovine urinary bladder combines the advantages of the in vivo animal model (high adequacy of the parietal surfaces) and the tissue fragments containing plastic container (low costs, easy handling and reproducibility, easy evaluation of technical factors and the absence of living animals).

There are various possibilities to further develop the method. A further series of experiments should be performed in a temperature level of 37°C. Additionally, electrostatic charges could be applied to investigate their influence on spray propagation and aerosol precipitation. The amount of deposited aerosol, which does not penetrate into the serosal tissue, could be weighted to obtain the exact degree of penetration.

4.1.2 Inverted bovine bladder model: limitations

Technical limitations appeared during the performing of the series of experiments. Some of the provided urinary bladders partly differed in diameter,

consistence, prestretching and width of neck aperture. Thus, bladders, which deviated to much from average had to be sorted out to ensure similar anatomical condition in all series of experiments.

Still, there are also certain issues, which have not been considered in this model, but are important to look at. The abdominal cavity is marked by various anatomical characteristics, which influence the distribution of a therapeutic aerosol significantly. There are regions, such as the spaces between neighboring bowel loops for example, which are hidden and not accessible easily by the aerosol, although the established capnoperitoneum leads to the formation of an arched abdominal cavity. These anatomical circumstances are not taken into account in the inverted bovine urinary bladder model.

4.1.3 Thermographic Imaging model

Classical field of applied Thermographic Imaging in medicinal context is the diagnosis of peripheral vascular diseases, skin, and breast cancer (Gurjarpadhye et al., 2015, Ring and Ammer, 2012).

So far, the Thermographic Imaging method has not been applied for scientific investigation of the distribution process in PIPAC research. In principle, the advantages of this method are multiform: the possibility of presenting the aerosol spreading process during injection phase and the droplet deposition during exposure phase in real-time. Furthermore, this technique is simple in handling, reproducible and cost-effective.

Special interest must be put in the real-time measurement. In all models published describing the aerosol distribution pattern (Solass et al., 2012b, Khosrawipour et al., 2016a, Khosrawipour et al., 2016b), only the result of application, as determined by tissue concentration, penetration depth and visual examination of stained serosa at the end of the period of exposition, was measured. Obviously, this has been a serious limitation, since aerosol distribution within a certain space is not static, but is subject to continuous changes. For example, due to gravitation forces, any aerosol regardless of optimal droplet size will deposit on the ground of the experiment model after a given period of time.

The Thermographic Imaging method is supposed to overcome this significant limitation by providing a continuous real-time analysis of the distribution pattern.

There are still limitations, the Thermographic Imaging model is suffering from.

First, the injection period (30sec) does not correspond to the duration in the operational setting (180sec) due to the special modalities of the experimental model box. Steady state conditions regarding heat transmission are attained after 30 sec.

Second, the exposure phase is not recorded due to technical limitations of the model box. A thermographic representation of the distribution behavior of the injected aerosol after the injection phase would be desirable to gain information about the sedimentation rate of the aerosol droplets over time. The materials used for the model box do not allow absorption of the aerosol droplets. Thus, it is inevitable that in the process of time, droplets form on the walls and the plastic wrap making longer observation of distribution behavior impossible. The deposited droplets on the front of the model box distort the received heat transmission, as the areas situated behind the droplets cannot be plotted representatively anymore. For this reason, the available experiment has high significance in analyzing both the spraying behavior of the examined Capnopen® and the aerosol distribution pattern during injection phase, but limitations in the examination of the absorption phase. A possible new approach to investigate the distribution pattern of an injected aerosol in the exposure phase over time would be to spray a contrast medium containing aerosol first into a model box and consecutively into the bladder model, which are located in a computed tomography scanner. In predefined time intervals, computed tomographic images should be taken with the aim of extrapolating from the density of the contrast medium in each spot in space to the distribution pattern of the exposed aerosol.

Third, the color (indicating amount of heat transmission) does not allow to draw explicit conclusions of the absolute concentration of the aerosol. Although there is a clear correlation between color and aerosol amount, it remains unclear, whether this correlation is proportional or not. For example, the red areas indicate, that the heat transmission is not disturbed by any aerosol droplets. After

beginning the injection, the area in the center of the box quickly turns yellow indicating less heat transmission caused by the appearance of aerosol droplets. Yet, one cannot draw any conclusion, whether just a very small number of droplets leads to the color change or a respectable amount is needed. The same issue appears later in the experiment. The color “blue” represents an enormous reduction of heat transmission. Again, it remains uncertain, how many droplets are responsible for the cooling of the area. Even a further concentration of aerosol might not lead to a significant change in heat transmission. To sum up, the available experiment points up relative changes in the heat transmission without making clear statements about the exact absolute amount of the distributed aerosol over time.

4.2 Evaluation of a next-generation medical device

To my knowledge, this dissertation is the first to deal with the comparison of distribution behavior of a drug containing solution in an experimental model between the Capnopen®, currently used as a standard in the operational setting, and the Prototype4, the newest generation. As an experimental model, the inverted bovine urinary bladder has been proved to be a valid possibility to mimic the abdominal cavity.

The proposed core element of effective PIPAC therapy is a homogenous drug distribution. Only through that, it can be guaranteed, that the drug (here in the experiments Methylene blue, ICG, DAPI and Cisplatin) can reach all target cells and unfold its full efficacy. As long as not all regions of the abdominal cavity (or as an experimental model the inverted bovine urinary bladder) are sufficiently covered with the drug containing solution, no effective or even curative therapeutic approach will be possible.

In a large series of experiments, two different medical devices (Capnopen® and Prototype4) were tested to carve out the granulometric aerosol characteristics, the spray propagation behaviour and the distribution and penetration pattern. As distribution within the abdominal cavity is still not ideal, the hypothesis was, that

a new medical device (Prototype4) with improved technical properties would lead to a more homogenous distribution.

In a first step, technical properties are revealed through granulometric and thermographic analysis.

4.2.1 Granulometric analysis

Granulometric analysis via Laser Diffraction to determine the droplet size distribution offers a good possibility to gain further information about the aerosol characteristics of both Capnopen®.

Two main aspects can be examined by means of the obtained granulometric data. First, the aerosol of Prototype4 is slightly more homogenous regarding droplet size distribution than of Capnopen®. Second, the range of droplet size diameters of both Capnopen® is comparatively small. 80 % of the entire aerosol volume consists of droplets with comparably similar size. Through that, the objective of a low dispersion of droplet diameters within the aerosol has become closer. This is beneficial for both less aerosol volume loss due to inertial impaction and a higher homogeneity within the aerosol. These characteristics rather apply for the aerosol of Prototype4 than for the Capnopen®.

In current research, there is discussion about the ideal droplet size for optimal homogenous drug distribution and effective penetration into the tissue. Various granulometric experiments have been carried out to define the current diameter distribution of the nebulizer. Khosrawipour et al described, that the Capnopen® sprays with a droplet diameter ranging from 3 – 15 µm (Khosrawipour et al., 2016a). In the granulometric analysis, Göhler et al revealed, that the size distribution is bimodal with one peak <3 µm and the other 10 – 15 µm. Similar results were achieved by another study (Reymond and Solass, 2014).

The findings in the present granulometric experiment are difficult to compare with the granulometric analysis of Göhler et al., as in their study, a completely different experimental set up had been established (different angioinjector, laser - diffraction spectrometer and a shorter distance between nozzle of the nebulizer to the laser beam) (Gohler et al., 2017).

4.2.2 Injection angle and distribution velocity

The performed series of experiments in the Thermographic Imaging model reveal certain advantages of the Prototype4 over the established Capnopen® regarding injection angle and aerosol velocity distribution.

First, the injection angle of the nozzle of the Prototype4 is wider with $\beta=55^\circ$. Through this technical characteristic, the injection jet is not only restricted to the central column of the box, but leads to a wider, more scattered distribution of the aerosol volume in space, so that the inertial impaction factor opposite to the nebulizer nozzle is less distinctive and more homogenous drug distribution can be achieved.

Second, the spreading of aerosol proceeds faster. Therefore, the model box is filled adequately earlier leading to a longer exposure phase.

In general, the spreading pattern of both devices is similar. The injection of the aerosol leads to a symmetrical distribution within the box. The process of filling runs of with coverage of the center of bottom first, followed by the entire ground and then moving progressively upwards, until the entire box is filled at the end of the thermographic recording. The upper central parts are aerosolized last. Both Capnopen® achieve sufficient filling with aerosol of the entire box after a predefined period.

4.2.3 Visual examination of distribution pattern

Methylene blue staining within the inverted bovine urinary bladder was the first distribution pattern analysis. Visual-qualitative examination revealed a considerable homogenous staining of the surfaces of the bladders with no substantial difference between the Capnopen® and the Prototype4. The obtained results are of limited value, as qualitative analysis via visual examination leaves a big margin in interpretation. Additionally, for Prototype4, only one experiment round was performed. Hence, these series of experiments served as proof of model concept only. By means of the methylene blue staining, the feasibility of

the experimental set up of the inverted bovine urinary bladder was tested successfully.

In the results of the Fluorescence Imaging method, no fundamental differences between the Capnopen® regarding the visual distribution pattern of ICG can be seen. All parts of the inverted bovine urinary bladders, independently from the used Capnopen®, are covered with ICG emitted fluorescence. The images of the Capnopen® even show a slightly more homogenous emission in comparison to Prototype4.

It is self-explanatory, that all parts of the bladders emitting ICG fluorescence light, must have been covered with the aerosol during the exposure time of 30 min. Yet, the recorded fluorescence light does not make any statement about the period of aerosol presence in the respective parts of the bladders, nor does it let extrapolate from the signal intensity level to the penetration depth into the serosal tissue. As only the emission of the tissue surface is recorded, deeper penetration does not result in more intense signal intensity level. This on-off principle limits the informative value of this method.

Another point of interest was to compare not only the differences in the fluorescence images between the two Capnopen®, but also to combine their distribution information with the results of the obtained results from the DAPI penetration depth measurements and evaluate if a positive correlation can be carved out.

Unfortunately, a direct connection between these two methods cannot be determined. In the analyses of fluorescence microscopy, the obtained penetration depth results of DAPI reveal a substantial increase in the respective low parts of the bladders. Furthermore, in general, the penetration depth values are higher with the Prototype4 than with the Capnopen®. These findings cannot be validated by the ICG fluorescence imaging method.

The ICG fluorescence imaging method suits for getting a first visual insight into the drug distribution pattern within the bladder, but lacks in analyzing the concrete penetration depth into tissue.

4.2.4 Penetration depths in inverted bovine urinary bladder model

The experiments, evaluating the penetration depth of DAPI into the serosal tissue of the inverted bovine urinary bladder, have revealed major differences between the Capnopen® and Prototype4. The penetration depths of Prototype4 created aerosols are clearly above those of the Capnopen® regardless of the investigated area.

Up to now, penetration depth investigations in different locations within an experimental model had always been disappointing showing unequal penetration depth values in the different regions. Even though these preclinical models suffered from various inadequacies, it is clear, that improvement towards a homogeneous distribution of penetration depth is necessary in the development of PIPAC technology.

Different aspects of the penetration depth measurements should be taken into consideration.

In scientific literature, only few penetration depth values of PIPAC technology are indicated. In tissue measurement of a postmortem swine model, the penetration depth of doxorubicin was found out to be up to 350 µm opposite of the nozzle of the nebulizer and remarkably lower in more distant corners of the abdominal cavity (Khosrawipour et al., 2016c). Solass et al reported a penetration depth of 500 – 600 µm into tumor and peritoneal tissue (Solass et al., 2014). Preclinical experiments using a plastic box with positioned tissue samples in predefined areas also showed a substantial difference in the penetration depth values depending on the location of the specimen. Only the samples situated closely to the nozzle of the nebulizer had a mean penetration depth of 200 - 300 µm, rapidly dropping under 100 µm on the sides and the top of the plastic box (Khosrawipour et al., 2016a).

For Capnopen®, median penetration depth values are 151, 243 and 459 µm for top, middle, and low region respectively. Overall, considering the values in an absolute manner, these values correspond to the findings the earlier published

studies. The median of 459 μm for the low region is comparable to the result of Solass et al of 500 – 600 μm , which reported doxorubicin penetration however.

Yet, differences exist regarding the values of the upper and lower part of the bladders. In the other studies, penetration depth values of more distant location to the spray jet were reported to be significantly lower than the maximum opposite of the nozzle. Here, the median values of 151 μm in the top and 243 μm in the middle are also lower, but do not fall below the limit of 100 μm .

For the new Prototype4, penetration depth values differ substantially from the previous findings in PIPAC research. Both the absolute values and the differences between the top, middle and low part values indicate an improved distribution pattern.

With a median value of 511 μm for the top region, the penetration depth is significantly higher. Also, the values of the middle and the low region of 755 and 644 μm respectively show a deeper penetration into the serosal tissue than both with the Capnopen® in the present experiments and in the other studies reported.

These findings can be explained by the improved characteristics of the aerosol created by the Prototype4 and the advantages of the new inverted bovine urinary bladder. In the analysis of the new Prototype4, the Thermographic Imaging analysis points out a wider injection angle of the nozzle and an increased velocity of aerosol propagation. The granulometric evaluation of droplet size distribution via Laser Diffraction reveals a more homogenous aerosol regarding droplet size distribution. Thus, these developed technical and granulometric characteristics of the aerosol created by the Prototype4 lead to an improved drug distribution pattern and consecutively, as explained in the following, to a deeper drug penetration into the serosal tissue.

Correlation between penetration depth and distribution pattern

There are two basic assumptions, which contribute to the understanding of the relation between penetration depth and distribution pattern.

First, the higher the concentration of a drug is in a certain area of the experimental model, the deeper it penetrates the tissue.

Second, the longer the exposure time, the deeper the penetration. Granted that the aerosol has distributed gas-like first, but then its droplets deposit on the ground after a short period, a reduced penetration depth in the upper parts and an increased in the lower parts will be the consequence.

Based on these two assumptions, one can extrapolate from the penetration depth to the distribution pattern of an aerosol.

A third mechanism of an elevated penetration depth must be noted. In the stream jet of the Capnopen®, the inertial impaction of the aerosol contributes to a higher penetration depth (Gohler et al., 2016). This just affects the region of the bladder opposite of the Capnopen® nozzle.

In a series of experiments, the penetration depth of DAPI into the tissue, aerosolized by Capnopen® and Prototype4, was investigated. The detailed listing of the penetration depth values can be found in the chapter “results”. The results reveal an uneven penetration depths distribution with highest values in the low part of the bladder. This is not too surprising due the fact, that after a certain period of time, the droplets deposit on the ground of the bladder due to gravitation forces. Furthermore, this region is located in the stream jets of both Capnopen®, so that during injection period, penetration into the tissue is be supported by inertial impaction (Gohler et al., 2016).

Yet, considerable differences between the penetration depth values of both Capnopen® can be recognized. For the Capnopen®, a clear discrepancy between the middle and the top parts on the one hand and the low part on the other hand can be identified regarding homogenous penetration depth distribution. These penetration depths can be interpreted as characteristics of the distribution pattern. As described above, deep penetration is caused by a high amount of drug in the particular space and a long exposure time.

By means of these considerations, one can draw the conclusion, that with the Capnopen®, the distribution pattern of DAPI within the inverted bovine urinary bladder is not homogenous, but heterogenous with focus on the bottom. Similar results regarding heterogenous drug distribution have already been published

(Khosrawipour et al., 2016a, Khosrawipour et al., 2016b, Khosrawipour et al., 2016c).

The penetration depths of Prototype4 are clearly above those of the Capnopen® regardless of the investigated area. Furthermore, the achieved penetration depth values in the middle come very close to those in the low part.

These values indicate an improved spatial drug distribution. Even in the top part of the bladder, a higher concentration of the aerosol seems to be established, leading to a higher penetration depth.

Compared to the distribution pattern of the Capnopen®, it can be clearly determined, that the distribution with Prototype4 is more homogenous.

Yet, it must be outlined, that for these statistical analyses, only three bladder experiments for each Capnopen® were carried out. Therefore, the results of the penetration depth distribution must be interpreted with caution. Further studies are necessary to confirm the superior qualities of the Prototype4.

4.3 Conclusion

Through various series of experiments (Methylene Blue staining, ICG/DAPI and Cisplatin injection), the inverted bovine urinary bladder model has been implemented successfully and regarded valid for further application. Results were reproducible and convincing.

In the further method development, different options appear legitimate. Electrodes could be placed on top and bottom. Through applying a voltage, the modified distribution pattern of the administered aerosol could be examined. This technique has been described before by Kakchekeeva et al (Kakchekeeva et al., 2016).

Another field of necessary further research is the presentation of the transient aerosol behavior in space over time. The Thermographic Imaging method has been shown to be able to present the aerosol injection phase in a model box in real-time. However, marks only first step in this important investigation field, as both the model (plastic box) and the passage of recording (only injection phase)

are not ideal yet. The more informative exposure phase could not be displayed due to technical restrictions. Therefore, either these limitations can be overcome or a new fundamental approach is needed. This could be for example the use of Computed-tomographic (CT) Imaging. The inverted bovine urinary bladder model could be placed in the CT. The distribution pattern of the aerosol, consisting of contrast medium, over time could be displayed by taking repeated CT scans in predefined time intervals.

The research results suggest a superior distribution pattern of the aerosol created by Prototype4. This could be confirmed by Thermographic Imaging, penetration depth measurements of DAPI in the inverted bovine urinary bladder. Yet, a completely homogenous drug distribution could not be described, there are still differences between the upper and the lower regions in the respective models.

One key element in the creation process of PIPAC technology is the nebulizer. The way, the drug containing solution is atomized into the aerosol decides upon the further distribution and subsequently penetration into tissue. In the presented series of experiments, aerosols, created by the Prototype4, had superior qualities regarding injection angle, spreading velocity, droplet size diameter homogeneity and approximating penetration depth values between the top and bottom regions. These findings should now be further evaluated in improved settings (environmental steering) and taken into account in the further technical development of the next Capnopen®.

Particular interest should be put in the steering of the environment. As already described in the introduction, there are two main paths, which are considered equally important in the creation process of the aerosol. Only if the technical devices and the drug containing solution are accurately coordinated, the administered aerosol will diffuse and penetrate the target tissue effectively. In this dissertation, focus has been put on the evaluation of the different generation of the Capnopen®. In further experiments, the impact of modified physico-chemical factors such as temperature, pressure and loading should be examined.

Various limiting factors in the experiment conception appeared during experiment implementations. In the inverted bovine urinary bladder experiments, a wide

variation of anomalies in the anatomy of the used bladders impeded the creation of exact comparable experimental set ups. It is natural, that no bovine urinary bladder is exact like the other. However, only bladders with comparable characteristics regarding diameter, consistence, prestretching and width of neck aperture were used.

In the ICG/DAPI series of experiments, for each of both Capnopen®, four bladders were investigated, in the Cisplatin experiments, three bladders only with Capnopen®. More series of experiments are now needed to confirm first obtained promising results.

5 Abstract

For a long time, PM has been considered to be a terminal clinical condition. Pressurized intraperitoneal aerosol chemotherapy (PIPAC) is an innovative therapeutic approach with the target to become a curative treatment. The chemotherapeutic drugs are not delivered anymore into the abdominal cavity by conventional lavage, but administered by means of a pressurized, chemotherapeutic drug containing aerosol. The objective is to achieve a homogeneous drug distribution within the abdominal cavity. Through the gaseous propagation of the chemotherapeutic drugs, every region, regardless of its proximity or distance to the nozzle of the nebulizer in the laparoscopic setting, is covered sufficiently. This is not attainable with conventional lavage, where the low abdominal regions are treated sufficiently due to gravitational forces, while the upper regions are less covered, resulting in ineffective cancer treatment, as not all tumor nodules are caught.

In the past, various in vivo, ex vivo and postmortem swine experiments have been made to describe and improve the distribution pattern of an injected aerosol and the penetration depth into the serosal tissue. However, theoretical considerations regarding homogenous drug distribution via aerosolized administration did not match with actual results. Drug propagation was found out to be heterogeneous. All presented models suffer from different limitations, such as difficult reproducibility of results, extensive costs, and high discrepancies between anatomical conditions and model setup. Therefore, in this dissertation, a new ex vivo preclinical model, the inverted bovine urinary bladder, has been introduced. Advantages of the inverted bovine urinary bladder include simple handling, cost effectiveness, effect evaluation of various substances both on the mucosa and the serosa, integration of the physico-chemical characteristics of the operational environment, and proximity to the abdominal anatomical conditions.

Additionally, so far, no model is able to cover the transient behavior of spray propagation. Therefore, a first dynamic experimental model, the Thermographic Imaging, has been established to describe the aerosol propagation within a model box during the injection period in real time. The presented Thermographic

Imaging model is able to characterize the spraying behavior of the inserted different nebulizers and the aerosol propagation behavior during injection phase, but due to technical restrictions is not applicable to the sedimentation process of the aerosol during the exposure period.

A further focus of this dissertation is the implementation of a series of experiments, in which aerosols are created via two different nebulizers (Capnopen® and Prototype4) and their distribution/penetration depth pattern is evaluated in these new established models.

First, a visual-qualitative proof of drug distribution in all parts of the bladder was conducted, observing the effect of injected dye methylene blue and ICG. This was enhanced with penetration depth measurements of injected DAPI in three predefined regions within the urinary bladder. Obtained data revealed relevant differences not only between the three different regions, but also between the investigated two Capnopen® types. The Prototype4 achieved superior penetration depth in total and a more homogenous distribution. In a third step, cisplatin, one of the chemotherapeutic drugs used in PIPAC technology, was aerosolized and tissue concentration in the same three locations measured. Obtained data confirm the findings of DAPI penetration depth measurements.

These series of experiments show impressively the need of optimizing both the technical, physical, and pharmacodynamic characteristics of the injected aerosol and the distribution pattern. The aerosol characteristics of the Prototype4 are superior in many ways. The combination of improved injection, more homogenous droplet size range, higher and more equally distributed penetration depth values and tissue concentration underlines the achieved aerosol improvement.

The inverted bovine urinary bladder turns out to be a valid model for the evaluation of the distribution pattern and penetration depth in the serosal tissue. In the future, these obtained promising results from the preclinical models should be transferred to the clinical operational setting.

6 Zusammenfassung (Deutsch)

Peritonealkarzinose wurde lange Zeit als klinischer Endzustand mit infauster Prognose angesehen. Druck-Aerosol-Chemotherapie (PIPAC) ist ein innovativer therapeutischer Ansatz mit der Zielsetzung, eine kurative Behandlungsform bei Peritonealkarzinose zu werden. Die chemotherapeutischen Wirkstoffe werden nicht mehr durch eine konventionelle Spülung in die Bauchhöhle, sondern mittels eines unter Druck stehenden, chemotherapeutisches Arzneimittel enthaltenden Aerosols eingebracht. Ziel ist es, eine homogene Medikamentenverteilung in der Bauchhöhle zu erreichen. Durch das gasförmige Verteilungsverhalten der Chemotherapeutika wird sollte jeder Bereich, unabhängig von seiner Entfernung zur Einspritzdüse, während der Laparoskopie ausreichend abgedeckt werden. Dies ist mit konventioneller Lavage nicht erreichbar, bei der die unteren Bauchbereiche aufgrund der Schwerkraft ausreichend behandelt werden, während die oberen Regionen weniger bedeckt sind, was zu einer ineffektiven Krebsbehandlung führt.

In der Vergangenheit wurden verschiedene In-vivo-, Ex-Vivo- und Postmortem-Schweine-Experimente durchgeführt, um das Verteilungsverhalten eines injizierten Aerosols und die Eindringtiefe in das Serosagewebe zu beschreiben und zu verbessern. Theoretische Überlegungen zur homogenen Verteilung von Medikamenten mittels Aerosolapplikation stimmten jedoch nicht mit den tatsächlichen Ergebnissen überein. Die Ausbreitung von Medikamenten erwies sich als heterogen. Alle vorgestellten Modelle unterliegen unterschiedlichen Einschränkungen, wie z. B. die schwierige Reproduzierbarkeit der Ergebnisse, hohe Kosten und hohe Diskrepanzen zwischen anatomischen Bedingungen und Modellaufbau. Daher wurde in dieser Dissertation ein neues präklinisches Ex-vivo-Modell, die invertierte Rinderharnblase, eingeführt. Die Vorteile dieses neuen Harnblasenmodells sind die einfache Handhabung, die Kosteneffizienz, die Untersuchung verschiedener Substanzen sowohl auf der Mukosa als auch auf der Serosa, die Möglichkeit einer Einbeziehung der physikalisch-chemischen

Eigenschaften der Operationsumgebung und die ähnlichen anatomischen Bedingungen zu denen eines menschlichen Abdomens.

Darüber hinaus kann bisher kein Modell das vorübergehende Ausbreitungsverhalten eines Aerosols in der Injektionsphase abdecken. Daher wurde ein erstes dynamisches Versuchsmodell, das Thermographic Imaging, entwickelt, um die Ausbreitung des Aerosols in einer Modellbox während der Injektionszeit in Echtzeit zu beschreiben. Das vorgestellte Thermographic Imaging Modell ist in der Lage, das Sprühverhalten der eingesetzten unterschiedlichen Vernebler und das Ausbreitungsverhalten von Aerosolen während der Injektionsphase darzustellen. Aufgrund technischer Einschränkungen ist es jedoch nicht auf den Sedimentationsprozess des Aerosols während der Expositionszeit anwendbar.

Zunächst wurde ein visuell-qualitativer Nachweis der Medikamentenverteilung in allen Teilen der Blase durchgeführt, wobei die Wirkung des injizierten Farbstoffs Methyleneblau und ICG beobachtet wurde. Durch Messungen der Eindringtiefe von injiziertem DAPI in drei vordefinierten Bereichen der Harnblase wurden diese ersten Eindrücke objektivierbar gemacht. Die gewonnenen Daten zeigten relevante Unterschiede nicht nur zwischen den drei verschiedenen Regionen, sondern auch zwischen den beiden untersuchten Capnopen®-Typen. Der Prototyp4 erreichte insgesamt eine größere Eindringtiefe und eine homogenere Verteilung. In einem dritten Schritt wurde Cisplatin, eines der in der PIPAC-Technologie verwendeten Chemotherapeutika, eingesprützt und die Gewebekonzentration an denselben drei Stellen gemessen. Die erhaltenen Daten bestätigen die Ergebnisse der DAPI-Eindringtiefmessungen.

Ein weiteres Hauptaugenmerk dieser Dissertation liegt in der Durchführung von mehreren Experimenten, in denen mittels zweier verschiedener Vernebler (Capnopen® und Prototyp4) Aerosole erzeugt werden, deren Verteilungsverhalten beziehungsweise Eindringtiefen in diesen neu erstellten Modellen untersucht werden.

Diese Versuchsreihen zeigen eindrucksvoll die Notwendigkeit, sowohl die technischen, physikalischen als auch die pharmakodynamischen Eigenschaften des injizierten Aerosols und das Verteilungsmuster zu optimieren. Die Aerosoleigenschaften des Prototype4 sind in vielerlei Hinsicht überlegen.

Die Kombination aus verbesserter Injektion, homogeneren Tröpfchengrößen, größerer und gleichmäßig verteilter Eindringtiefe und Gewebekonzentration unterstreicht die erzielte Verbesserung des Aerosols.

Es hat sich gezeigt, dass die invertierte Rinderharnblase ein valides Modell für die Bewertung des Verteilungsmusters und der Eindringtiefe in das Serosagewebe darstellt. In der Zukunft sollten diese vielversprechenden Ergebnisse aus den präklinischen Modellen in den klinischen Alltag übertragen werden.

7 References

- ALANDER, J. T., KAARTINEN, I., LAAKSO, A., TIL, T., SPILLMANN, T., TUCHIN, V. V., VENERMO, M., & LISUO, P. 2012. A Review of Indocyanine Green Fluorescent Imaging in Surgery. *International Journal of Biomedical Imaging*, 2012, 26.
- ALBANESE, A. M., ALBANESE, E. F., MINO, J. H., GOMEZ, E., GOMEZ, M., ZANDOMENI, M. & MERLO, A. B. 2009. Peritoneal surface area: measurements of 40 structures covered by peritoneum: correlation between total peritoneal surface area and the surface calculated by formulas. *Surg Radiol Anat*, 31, 369-77.
- ALIJANI, A., HANNA, G. B. & CUSCHIERI, A. 2004. Abdominal wall lift versus positive-pressure capnoperitoneum for laparoscopic cholecystectomy: randomized controlled trial. *Ann Surg*, 239, 388-94.
- BECKERT, S., STRULLER, F., GRISCHKE, E. M., GLATZLE, J., ZIEKER, D., KONIGSRAINER, A. & KONIGSRAINER, I. 2016. [Surgical Management of Peritoneal Surface Malignancy with Respect to Tumour Type, Tumour Stage and Individual Tumour Biology]. *Zentralbl Chir*, 141, 415-20.
- BLANCO, A., GIGER-PABST, U., SOLASS, W., ZIEREN, J. & REYMOND, M. A. 2013. Renal and hepatic toxicities after pressurized intraperitoneal aerosol chemotherapy (PIPAC). *Ann Surg Oncol*, 20, 2311-6.
- BRITANNICA, T. E. O. E. April 11, 2016. *Stokes's law* [Online]. <https://www.britannica.com/science/Stokess-law>: Encyclopædia Britannica, inc. . [Accessed 04/07/2017 2017].
- CARVALHO, C., SANTOS, R. X., CARDOSO, S., CORREIA, S., OLIVEIRA, P. J., SANTOS, M. S. & MOREIRA, P. I. 2009. Doxorubicin: the good, the bad and the ugly effect. *Curr Med Chem*, 16, 3267-85.
- CAZAURAN, J. B., ALYAMI, M., LASSEUR, A., GYBELS, I., GLEHEN, O. & BAKRIN, N. 2018. Pressurized Intraperitoneal Aerosol Chemotherapy (PIPAC) Procedure for Non-resectable Peritoneal Carcinomatosis (with Video). *J Gastrointest Surg*, 22, 374-375.
- CAZZOLA, M., PAGE, C. P., CALZETTA, L. & MATERA, M. G. 2012. Pharmacology and therapeutics of bronchodilators. *Pharmacol Rev*, 64, 450-504.
- CEELEN, W. P. & FLESSNER, M. F. 2010. Intraperitoneal therapy for peritoneal tumors: biophysics and clinical evidence. *Nat Rev Clin Oncol*, 7, 108-15.
- CHU, D. Z., LANG, N. P., THOMPSON, C., OSTEEN, P. K. & WESTBROOK, K. C. 1989. Peritoneal carcinomatosis in nongynecologic malignancy. A prospective study of prognostic factors. *Cancer*, 63, 364-7.
- CHUA, T. C., YAN, T. D. & MORRIS, D. L. 2009. Surgical biology for the clinician: peritoneal mesothelioma: current understanding and management. *Can J Surg*, 52, 59-64.
- DE CUBA, E. M., KWAKMAN, R., KNOL, D. L., BONJER, H. J., MEIJER, G. A. & TE VELDE, E. A. 2013. Cytoreductive surgery and HIPEC for peritoneal metastases combined with curative treatment of colorectal liver metastases: Systematic review of all literature and meta-analysis of observational studies. *Cancer Treat Rev*, 39, 321-7.
- DEDRICK, R. L. & FLESSNER, M. F. 1997. Pharmacokinetic problems in peritoneal drug administration: tissue penetration and surface exposure. *J Natl Cancer Inst*, 89, 480-7.
- DEMTRODER, C., SOLASS, W., ZIEREN, J., STRUMBERG, D., GIGER-PABST, U. & REYMOND, M. A. 2016. Pressurized intraperitoneal aerosol chemotherapy with oxaliplatin in colorectal peritoneal metastasis. *Colorectal Dis*, 18, 364-71.
- DEMYTTENAERE, S., FELDMAN, L. S. & FRIED, G. M. 2007. Effect of pneumoperitoneum on renal perfusion and function: a systematic review. *Surg Endosc*, 21, 152-60.

- DICTIONARY, T. A. H. S. Juli 2017. "Aerosol," in *The American Heritage® Science Dictionary*. Source location: Houghton Mifflin Company. <http://www.dictionary.com/browse/aerosol>. Accessed: July 4, 2017 10:15 [Online]. <http://www.dictionary.com/browse/aerosol>: Houghton Mifflin Company. [Accessed].
- DOS SANTOS, N. A., CARVALHO RODRIGUES, M. A., MARTINS, N. M. & DOS SANTOS, A. C. 2012. Cisplatin-induced nephrotoxicity and targets of nephroprotection: an update. *Arch Toxicol*, 86, 1233-50.
- EMOTO, S., ISHIGAMI, H., HIDEMURA, A., YAMAGUCHI, H., YAMASHITA, H., KITAYAMA, J. & WATANABE, T. 2012. Complications and management of an implanted intraperitoneal access port system for intraperitoneal chemotherapy for gastric cancer with peritoneal metastasis. *Jpn J Clin Oncol*, 42, 1013-9.
- ESQUIS, P., CONSOLO, D., MAGNIN, G., POINTAIRE, P., MORETTO, P., YNSA, M. D., BELTRAMO, J. L., DROGOUL, C., SIMONET, M., BENOIT, L., RAT, P. & CHAUFFERT, B. 2006. High intra-abdominal pressure enhances the penetration and antitumor effect of intraperitoneal cisplatin on experimental peritoneal carcinomatosis. *Ann Surg*, 244, 106-12.
- FACY, O., AL SAMMAN, S., MAGNIN, G., GHIRINGHELLI, F., LADOIRE, S., CHAUFFERT, B., RAT, P. & ORTEGA-DEBALLON, P. 2012. High pressure enhances the effect of hyperthermia in intraperitoneal chemotherapy with oxaliplatin: an experimental study. *Ann Surg*, 256, 1084-8.
- FRANKO, J., SHI, Q., MEYERS, J. P., MAUGHAN, T. S., ADAMS, R. A., SEYMOUR, M. T., SALTZ, L., PUNT, C. J. A., KOOPMAN, M., TOURNIGAND, C., TEBBUTT, N. C., DIAZ-RUBIO, E., SOUGLAKOS, J., FALCONE, A., CHIBAUDEL, B., HEINEMANN, V., MOEN, J., DE GRAMONT, A., SARGENT, D. J. & GROTHEY, A. 2016. Prognosis of patients with peritoneal metastatic colorectal cancer given systemic therapy: an analysis of individual patient data from prospective randomised trials from the Analysis and Research in Cancers of the Digestive System (ARCAD) database. *Lancet Oncol*, 17, 1709-1719.
- GAROFALO, A., VALLE, M., GARCIA, J. & SUGARBAKER, P. H. 2006. Laparoscopic intraperitoneal hyperthermic chemotherapy for palliation of debilitating malignant ascites. *Eur J Surg Oncol*, 32, 682-5.
- GIGER-PABST, U., DEMTRODER, C., FALKENSTEIN, T. A., OUAISSI, M., GOTZE, T. O., REZNICZEK, G. A. & TEMPFER, C. B. 2018. Pressurized IntraPeritoneal Aerosol Chemotherapy (PIPAC) for the treatment of malignant mesothelioma. *BMC Cancer*, 18, 442.
- GIGER-PABST, U., SOLASS, W., BUERKLE, B., REYMOND, M. A. & TEMPFER, C. B. 2015. Low-dose pressurized intraperitoneal aerosol chemotherapy (PIPAC) as an alternative therapy for ovarian cancer in an octogenarian patient. *Anticancer Res*, 35, 2309-14.
- GILL, R. S., AL-ADRA, D. P., NAGENDRAN, J., CAMPBELL, S., SHI, X., HAASE, E. & SCHILLER, D. 2011. Treatment of gastric cancer with peritoneal carcinomatosis by cytoreductive surgery and HIPEC: a systematic review of survival, mortality, and morbidity. *J Surg Oncol*, 104, 692-8.
- GIRSHALLY, R., DEMTRODER, C., ALBAYRAK, N., ZIEREN, J., TEMPFER, C. & REYMOND, M. A. 2016. Pressurized intraperitoneal aerosol chemotherapy (PIPAC) as a neoadjuvant therapy before cytoreductive surgery and hyperthermic intraperitoneal chemotherapy. *World J Surg Oncol*, 14, 253.
- GOHLER, D., KHOSRAWIPOUR, V., KHOSRAWIPOUR, T., DIAZ-CARBALLO, D., FALKENSTEIN, T. A., ZIEREN, J., STINTZ, M. & GIGER-PABST, U. 2016. Technical description of the microinjection pump (MIP(R)) and granulometric characterization of the aerosol applied for pressurized intraperitoneal aerosol chemotherapy (PIPAC). *Surg Endosc*.
- GOHLER, D., KHOSRAWIPOUR, V., KHOSRAWIPOUR, T., DIAZ-CARBALLO, D., FALKENSTEIN, T. A., ZIEREN, J., STINTZ, M. & GIGER-PABST, U. 2017. Technical description of the microinjection pump (MIP(R)) and granulometric characterization of the aerosol applied

- for pressurized intraperitoneal aerosol chemotherapy (PIPAC). *Surg Endosc*, 31, 1778-1784.
- GRASS, F., VUAGNIAUX, A., TEIXEIRA-FARINHA, H., LEHMANN, K., DEMARTINES, N. & HUBNER, M. 2017. Systematic review of pressurized intraperitoneal aerosol chemotherapy for the treatment of advanced peritoneal carcinomatosis. *Br J Surg*, 104, 669-678.
- GRIFFITHS, R. W., ZEE, Y. K., EVANS, S., MITCHELL, C. L., KUMARAN, G. C., WELCH, R. S., JAYSON, G. C., CLAMP, A. R. & HASAN, J. 2011. Outcomes after multiple lines of chemotherapy for platinum-resistant epithelial cancers of the ovary, peritoneum, and fallopian tube. *Int J Gynecol Cancer*, 21, 58-65.
- GUERRERO, Y., SINGH, S., MAI, T., MURALI, R., TANIKELLA, L., ZAHEDI, A., KUNDRU, V. & ANVARI, B. 2017. Optical Characteristics and Tumor Imaging Capabilities of Near Infrared Dyes in Free and Nano-Encapsulated Formulations Comprised of Viral Capsids. *ACS Appl Mater Interfaces*.
- GURJARPADHYE, A. A., PAREKH, M. B., DUBNIKA, A., RAJADAS, J. & INAYATHULLAH, M. 2015. Infrared Imaging Tools for Diagnostic Applications in Dermatology. *SM J Clin Med Imaging*, 1, 1-5.
- HALKIA, E., GAVRIEL, S. & SPILIOTIS, J. 2014. Management of peritoneal surface malignancy: a review of the recent literature. *J buon*, 19, 618-26.
- HANDGRAAF, H. J. M., BOOGERD, L. S. F., HOPPENER, D. J., PELOSO, A., SIBINGA MULDER, B. G., HOOGSTINS, C. E. S., HARTGRINK, H. H., VAN DE VELDE, C. J. H., MIEOG, J. S. D., SWIJNENBURG, R. J., PUTTER, H., MAESTRI, M., BRAAT, A. E., FRANGIONI, J. V. & VAHRMEIJER, A. L. 2017. Long-term follow-up after near-infrared fluorescence-guided resection of colorectal liver metastases: A retrospective multicenter analysis. *Eur J Surg Oncol*.
- HANKER, L. C., LOIBL, S., BURCHARDI, N., PFISTERER, J., MEIER, W., PUJADE-LAURINE, E., RAYCOQUARD, I., SEHOULI, J., HARTER, P. & DU BOIS, A. 2012. The impact of second to sixth line therapy on survival of relapsed ovarian cancer after primary taxane/platinum-based therapy. *Ann Oncol*, 23, 2605-12.
- HELDIN, C. H., RUBIN, K., PIETRAS, K. & OSTMAN, A. 2004. High interstitial fluid pressure - an obstacle in cancer therapy. *Nat Rev Cancer*, 4, 806-13.
- JACQUET, P., STUART, O. A., CHANG, D. & SUGARBAKER, P. H. 1996. Effects of intra-abdominal pressure on pharmacokinetics and tissue distribution of doxorubicin after intraperitoneal administration. *Anticancer Drugs*, 7, 596-603.
- JAYNE, D. G., FOOK, S., LOI, C. & SEOW-CHOEN, F. 2002. Peritoneal carcinomatosis from colorectal cancer. *Br J Surg*, 89, 1545-50.
- KAKCHEKEEVA, T., DEMTRODER, C., HERATH, N. I., GRIFFITHS, D., TORKINGTON, J., SOLASS, W., DUTREIX, M. & REYMOND, M. A. 2016. In Vivo Feasibility of Electrostatic Precipitation as an Adjunct to Pressurized Intraperitoneal Aerosol Chemotherapy (ePIPAC). *Ann Surg Oncol*.
- KAPUSCINSKI, J. 1995. DAPI: a DNA-Specific Fluorescent Probe. *Biotechnic & Histochemistry*, 70, 220-233.
- KHOSRAWIPOUR, V., KHOSRAWIPOUR, T., DIAZ-CARBALLO, D., FORSTER, E., ZIEREN, J. & GIGER-PABST, U. 2016a. Exploring the Spatial Drug Distribution Pattern of Pressurized Intraperitoneal Aerosol Chemotherapy (PIPAC). *Ann Surg Oncol*, 23, 1220-4.
- KHOSRAWIPOUR, V., KHOSRAWIPOUR, T., FALKENSTEIN, T. A., DIAZ-CARBALLO, D., FORSTER, E., OSMA, A., ADAMIETZ, I. A., ZIEREN, J. & FAKHRIAN, K. 2016b. Evaluating the Effect of Micropump(c) Position, Internal Pressure and Doxorubicin Dosage on Efficacy of Pressurized Intra-peritoneal Aerosol Chemotherapy (PIPAC) in an Ex Vivo Model. *Anticancer Res*, 36, 4595-600.

- KHOSRAWIPOUR, V., KHOSRAWIPOUR, T., KERN, A. J., OSMA, A., KABAKCI, B., DIAZ-CARBALLO, D., FORSTER, E., ZIEREN, J. & FAKHRIAN, K. 2016c. Distribution pattern and penetration depth of doxorubicin after pressurized intraperitoneal aerosol chemotherapy (PIPAC) in a postmortem swine model. *J Cancer Res Clin Oncol*.
- LOSA, F., BARRIOS, P., SALAZAR, R., TORRES-MELERO, J., BENAVIDES, M., MASSUTI, T., RAMOS, I. & ARANDA, E. 2014. Cytoreductive surgery and intraperitoneal chemotherapy for treatment of peritoneal carcinomatosis from colorectal origin. *Clin Transl Oncol*, 16, 128-40.
- MARKMAN, M. 2003. Intraperitoneal antineoplastic drug delivery: rationale and results. *Lancet Oncol*, 4, 277-83.
- MARMOR, R. A., KELLY, K. J., LOWY, A. M. & BAUMGARTNER, J. M. 2016. Laparoscopy is Safe and Accurate to Evaluate Peritoneal Surface Metastasis Prior to Cytoreductive Surgery. *Ann Surg Oncol*, 23, 1461-7.
- MINCHINTON, A. I. & TANNOCK, I. F. 2006. Drug penetration in solid tumours. *Nat Rev Cancer*, 6, 583-92.
- NADIRADZE, G., GIGER-PABST, U., ZIEREN, J., STRUMBERG, D., SOLASS, W. & REYMOND, M. A. 2016. Pressurized Intraperitoneal Aerosol Chemotherapy (PIPAC) with Low-Dose Cisplatin and Doxorubicin in Gastric Peritoneal Metastasis. *J Gastrointest Surg*, 20, 367-73.
- NOWACKI, M., ALYAMI, M., VILLENEUVE, L., MERCIER, F., HUBNER, M., WILLAERT, W., CELEN, W., REYMOND, M., PEZET, D., ARVIEUX, C., KHOMYAKOV, V., LAY, L., GIANNI, S., ZEGARSKI, W., BAKRIN, N. & GLEHEN, O. 2018. Multicenter comprehensive methodological and technical analysis of 832 pressurized intraperitoneal aerosol chemotherapy (PIPAC) interventions performed in 349 patients for peritoneal carcinomatosis treatment: An international survey study. *Eur J Surg Oncol*, 44, 991-996.
- ODENDAHL, K., SOLASS, W., DEMTRODER, C., GIGER-PABST, U., ZIEREN, J., TEMPFER, C. & REYMOND, M. A. 2015. Quality of life of patients with end-stage peritoneal metastasis treated with Pressurized IntraPeritoneal Aerosol Chemotherapy (PIPAC). *Eur J Surg Oncol*, 41, 1379-85.
- PADILLA-VALVERDE, D., SANCHEZ-GARCIA, S., GARCIA-SANTOS, E., MARCOTE-IBANEZ, C., MOLINA-ROBLES, M., MARTIN-FERNANDEZ, J. & VILLAREJO-CAMPOS, P. 2016. Usefulness of Thermographic Analysis to Control Temperature Homogeneity in the Development and Implementation of a Closed Recirculating CO2 Chemohyperthermia Model. *Int J Hyperthermia*, 1-19.
- REYMOND, M. A., HU, B., GARCIA, A., RECK, T., KOCKERLING, F., HESS, J. & MOREL, P. 2000. Feasibility of therapeutic pneumoperitoneum in a large animal model using a microvaporisator. *Surg Endosc*, 14, 51-5.
- REYMOND, M. A. & SOLASS, W. 2014. *PIPAC - Pressurized Intraperitoneal Aerosol Chemotherapy - cancer under pressure*, De Gruyter.
- RING, E. F. & AMMER, K. 2012. Infrared thermal imaging in medicine. *Physiol Meas*, 33, R33-46.
- RIVERA, F., VEGA-VILLEGAS, M. E. & LOPEZ-BREA, M. F. 2007. Chemotherapy of advanced gastric cancer. *Cancer Treat Rev*, 33, 315-24.
- ROBELLA, M., VAIRA, M. & DE SIMONE, M. 2016. Safety and feasibility of pressurized intraperitoneal aerosol chemotherapy (PIPAC) associated with systemic chemotherapy: an innovative approach to treat peritoneal carcinomatosis. *World J Surg Oncol*, 14, 128.
- ROSSI, C. R., MOCELLIN, S., PILATI, P., FOLETTTO, M., QUINTIERI, L., PALATINI, P. & LISE, M. 2003. Pharmacokinetics of intraperitoneal cisplatin and doxorubicin. *Surg Oncol Clin N Am*, 12, 781-94.
- RUBIN, B. K. 2010. Air and soul: the science and application of aerosol therapy. *Respir Care*, 55, 911-21.

- SABAPATHY V, M. J., JACOB PM, KUMAR S. 2015. Noninvasive Optical Imaging and In Vivo Cell Tracking of Indocyanine Green Labeled Human Stem Cells Transplanted at Superficial or In-Depth Tissue of SCID Mice. . *Stem Cells International*.
- SANCHEZ-GARCIA, S., PADILLA-VALVERDE, D., VILLAREJO-CAMPOS, P., MARTIN-FERNANDEZ, J., GARCIA-ROJO, M. & RODRIGUEZ-MARTINEZ, M. 2014. Experimental development of an intra-abdominal chemohyperthermia model using a closed abdomen technique and a PRS-1.0 Combat CO2 recirculation system. *Surgery*, 155, 719-25.
- SCHILLING, M. K., REDAELLI, C., KRAHENBUHL, L., SIGNER, C. & BUCHLER, M. W. 1997. Splanchnic microcirculatory changes during CO2 laparoscopy. *J Am Coll Surg*, 184, 378-82.
- SCHNELLE, D., WEINREICH, F.-J., KIBAT, J. & REYMOND MARC, A. 2017. A new ex vivo model for optimizing distribution of therapeutic aerosols: the (inverted) bovine urinary bladder. *Pleura and Peritoneum*.
- SOLASS, W., HERBETTE, A., SCHWARZ, T., HETZEL, A., SUN, J. S., DUTREIX, M. & REYMOND, M. A. 2012a. Therapeutic approach of human peritoneal carcinomatosis with Dbait in combination with capnoperitoneum: proof of concept. *Surg Endosc*, 26, 847-52.
- SOLASS, W., HETZEL, A., NADIRADZE, G., SAGYNALIEV, E. & REYMOND, M. A. 2012b. Description of a novel approach for intraperitoneal drug delivery and the related device. *Surg Endosc*, 26, 1849-55.
- SOLASS, W., KERB, R., MURDTER, T., GIGER-PABST, U., STRUMBERG, D., TEMPFER, C., ZIEREN, J., SCHWAB, M. & REYMOND, M. A. 2014. Intraperitoneal chemotherapy of peritoneal carcinomatosis using pressurized aerosol as an alternative to liquid solution: first evidence for efficacy. *Ann Surg Oncol*, 21, 553-9.
- SOLASS, W., STRULLER, F., HORVATH, P., KÖNIGSRÄINER, A., SIPOS, B. & WEINREICH, F.-J. 2016. Morphology of the peritoneal cavity and pathophysiological consequences. *Pleura and Peritoneum*.
- SUGARBAKER, P. H. 1996. Observations concerning cancer spread within the peritoneal cavity and concepts supporting an ordered pathophysiology. *Cancer Treat Res*, 82, 79-100.
- SUGARBAKER, P. H. 2016. Cytoreductive surgery and hyperthermic intraperitoneal chemotherapy in the management of gastrointestinal cancers with peritoneal metastases: Progress toward a new standard of care. *Cancer Treat Rev*, 48, 42-9.
- SUGARBAKER, P. H. & JABLONSKI, K. A. 1995. Prognostic features of 51 colorectal and 130 appendiceal cancer patients with peritoneal carcinomatosis treated by cytoreductive surgery and intraperitoneal chemotherapy. *Ann Surg*, 221, 124-32.
- TEMPFER, C. B., CELIK, I., SOLASS, W., BUERKLE, B., PABST, U. G., ZIEREN, J., STRUMBERG, D. & REYMOND, M. A. 2014a. Activity of Pressurized Intraperitoneal Aerosol Chemotherapy (PIPAC) with cisplatin and doxorubicin in women with recurrent, platinum-resistant ovarian cancer: preliminary clinical experience. *Gynecol Oncol*, 132, 307-11.
- TEMPFER, C. B., GIGER-PABST, U., SEEBACHER, V., PETERSEN, M., DOGAN, A. & REZNICZEK, G. A. 2018. A phase I, single-arm, open-label, dose escalation study of intraperitoneal cisplatin and doxorubicin in patients with recurrent ovarian cancer and peritoneal carcinomatosis. *Gynecol Oncol*, 150, 23-30.
- TEMPFER, C. B., REZNICZEK, G. A., ENDE, P., SOLASS, W. & REYMOND, M. A. 2015a. Pressurized Intraperitoneal Aerosol Chemotherapy with Cisplatin and Doxorubicin in Women with Peritoneal Carcinomatosis: A Cohort Study. *Anticancer Res*, 35, 6723-9.
- TEMPFER, C. B., SOLASS, W., BUERKLE, B. & REYMOND, M. A. 2014b. Pressurized intraperitoneal aerosol chemotherapy (PIPAC) with cisplatin and doxorubicin in a woman with pseudomyxoma peritonei: A case report. *Gynecol Oncol Rep*, 10, 32-5.
- TEMPFER, C. B., WINNEKENDONK, G., SOLASS, W., HORVAT, R., GIGER-PABST, U., ZIEREN, J., REZNICZEK, G. A. & REYMOND, M. A. 2015b. Pressurized intraperitoneal aerosol

- chemotherapy in women with recurrent ovarian cancer: A phase 2 study. *Gynecol Oncol*, 137, 223-8.
- VAN DE VAART, P. J., VAN DER VANGE, N., ZOETMULDER, F. A., VAN GOETHEM, A. R., VAN TELLINGEN, O., TEN BOKKEL HUIJINK, W. W., BEIJNEN, J. H., BARTELINK, H. & BEGG, A. C. 1998. Intraperitoneal cisplatin with regional hyperthermia in advanced ovarian cancer: pharmacokinetics and cisplatin-DNA adduct formation in patients and ovarian cancer cell lines. *Eur J Cancer*, 34, 148-54.
- WEBER, T., ROITMAN, M. & LINK, K. H. 2012. Current status of cytoreductive surgery with hyperthermic intraperitoneal chemotherapy in patients with peritoneal carcinomatosis from colorectal cancer. *Clin Colorectal Cancer*, 11, 167-76.
- WEST, N. P., HOHENBERGER, W., WEBER, K., PERRAKIS, A., FINAN, P. J. & QUIRKE, P. 2010. Complete mesocolic excision with central vascular ligation produces an oncologically superior specimen compared with standard surgery for carcinoma of the colon. *J Clin Oncol*, 28, 272-8.

8 Declaration of authorship

Die Arbeit wurde in der Chirurgischen Universitätsklinik Tübingen, Klinik für Allgemein-, Viszeral- und Transplantationschirurgie unter der Betreuung von Herrn Prof. Dr. med. Alfred Königsrainer sowie unter der wissenschaftlichen Anleitung durch Herrn Prof. Dr. med. Marc Reymond durchgeführt.

Die Konzeption der Studie erfolgte durch Herrn Prof. Dr. Marc Reymond, Klinik für Allgemein-, Viszeral- und Transplantationschirurgie des Universitätsklinikums Tübingen.

Hiermit erkläre ich, Daniel Patrick Schnelle, dass ich die vorgelegte Dissertationsschrift „Optimization of the spatial distribution of a therapeutic pressurized aerosol (PIPAC): an ex-vivo study“ selbstständig und ohne unzulässige fremde Hilfe verfasst habe, keine anderen als die ausdrücklich bezeichneten Quellen und Hilfsmittel verwendet habe und wörtlich oder inhaltlich übernommene Stellen von mir als solche gekennzeichnet wurden.

Die Konzeption der apparativen Untersuchungen erfolgte durch mich. Bei der Durchführung unterstützen mich Herr Dr. hum. biol. Jürgen Weinreich, Frau Dr. med. Wiebke Solass, Herr Prof. Dr. Marc Reymond sowie Frau Anita Hack.

Die Datenauswertung lag in meiner Verantwortung, unterstützt wurde ich durch dabei durch Herrn Dr. hum. biol. Jürgen Weinreich und Frau Dr. med. Wiebke Solass.

Bei der Verfassung der Veröffentlichung: „A new ex vivo model for optimizing drug delivery with PIPAC: the (inverted) bovine urinary bladder“ waren folgende Personen beteiligt: Herr Dr. hum. biol. Jürgen Weinreich, Herr Janek Kibat sowie Herr Prof. Dr. med. Marc Reymond.

Tübingen, den 15.05.2019

Ort, Datum

Daniel Schnelle

9 Publications

Teile der vorliegenden Dissertation wurden bereits in folgender Publikation veröffentlicht:

Schnelle D, Weinreich FJ, Kibat J, Reymond MA 2017

A new ex vivo model for optimizing distribution of therapeutic aerosols: the (inverted) bovine urinary bladder. *Pleura Peritoneum*. 2017 Mar 1;2(1):37-41. doi: 10.1515/pp-2017-0006. Epub 2017 Mar 11.

10 Acknowledgement

Ich möchte mich herzlich bei Prof. Dr. med. Alfred Königsrainer für die interessante Aufgabe, und die Möglichkeit der spannenden wissenschaftlichen Mitarbeit sowie Bereitstellung der Mittel zur Durchführung bedanken.

Für die Betreuung der Dissertation möchte ich mich außerdem ganz herzlich bei Prof. Dr. med. Marc Reymond bedanken. Die gemeinsame Arbeit unter seiner Betreuung gab mir die Möglichkeit, einen tiefen Einblick in die klinische Forschung zu bekommen. Ich hatte selbst die Möglichkeit, mich aktiv daran zu beteiligen. Die Arbeit in seiner Arbeitsgruppe war spannend und ich fühlte mich als Doktorand sehr wertgeschätzt.

Besonders bedanken möchte ich mich zudem bei Dr. hum. biol. Jürgen Weinreich für die wissenschaftliche Mitbetreuung, die hilfreichen fachlichen Anregungen und zielorientierten Lösungsvorschläge.

Ein großer Dank gilt zudem meinen Eltern, die durch Korrekturlesen und motivierende Ratschläge viel zum Gelingen der Dissertation beigetragen haben.